A Tutorial on Wavelets from an Electrical Engineering Perspective, Part 1: Discrete Wavelet Techniques[1]

T. K. Sarkar[1], C. Su[1], R. Adve[1], M. Salazar-Palma[2], L. Garcia-Castillo[2], Rafael R. Boix[3]

[1]Department of Electrical and Computer Engineering
Syracuse University
121 Link Hall
Syracuse, New York 13244-1240 USA
Tel: +1 (315) 443-3775
Fax: +1 (315) 443-4441
E-mail: tksarkar@mailbox.syr.edu
Web: http://web.syr.edu/~tksarkar

[2]Dept. Senales and Sistemas
Polytechnique University of Madrid
28040 Madrid
Spain
E-mail: salazar@gmr.ssr.upm.es

[3]Dept. Electronica y Electromagnetismo
Universidad de Sevilla
41012 - Sevilla
Spain

Keywords: Wavelets, wavelet transforms, filters, matrix equations, operators

1. Abstract

The objective of this paper is to present the subject of wavelets from a filter-theory perspective, which is quite familiar to electrical engineers. Such a presentation provides both physical and mathematical insights into the problem. It is shown that taking the discrete wavelet transform of a function is equivalent to filtering it by a bank of constant-Q filters, the non-overlapping bandwidths of which differ by an octave. The discrete wavelets are presented, and a recipe is provided for generating such entities. One of the goals of this tutorial is to illustrate how the wavelet decomposition is carried out, starting from the fundamentals, and how the scaling functions and wavelets are generated from the filter-theory perspective. Examples are presented to illustrate the class of problems for which the discrete wavelet techniques are ideally suited. It is interesting to note that it is not necessary to generate the wavelets or the scaling functions in order to implement the discrete wavelet transform. Finally, it is shown how wavelet techniques can be used to solve operator/matrix equations. It is shown that the "orthogonal-transform property" of the discrete wavelet techniques does not hold in numerical computations.

[1]This is part 1 of a two-part article. Part 2, which treats the continuous case, will appear in the December issue.

2. Introduction

Many books and numerous papers have been published describing wavelets. It is not possible for us to include all the references. Selected references [1-3] have been chosen to illustrate where additional materials are available. No attempt has been made to provide the earliest reference material.

Wavelets are a set of functions that can be used effectively in a number of situations, to represent natural, highly transient phenomena that result from a dilation and shift of the original waveform. For example, when a pulse propagates through a layered medium, due to dispersion and for different electrical properties of the layers, the pulse is dilated and delayed, due to the finite velocity of propagation. The application of wavelets (which literally translates from *ondellets* in French into English as *small waves*) was first made in the area of geophysics [4], in 1980, by the French geophysicist J. Morlet, of Elf-Aquitane. A good history from the mathematical perspective is available in the special issue of the *IEEE Proceedings* [5].

In electrical engineering [6-8], however, wavelets have been popular for some time, under the various names of multirate sampling, quadrature-mirror filters, and so on. Since the majority of the readers of this article are assumed to have an electrical-engineering background, it will perhaps be useful to describe the methodology in terms of filter theory. One of the objectives is to illustrate that performing the discrete wavelet transform is equivalent to filtering a signal by a band of constant-Q filters, the non-overlapping bandwidths of which differ by an octave. It is hoped that this mode of presentation will make wavelets easier to visualize, conceptualize, and apply to the problem at hand–if the wavelet theory is relevant!

One of the goals of this paper is to illustrate how one can generate the scaling functions and the wavelets, specially tailored to one's needs.

Consider a signal, $x(t)$, the Fourier transform of which is $X(\omega)$. In this paper, we deal only with discrete wavelet techniques. Discrete wavelet techniques are quite suitable for discrete signal processing, for example, in speech and image processing. In particular, their applications are very desirable in data compression. Since a complex matrix is a two-dimensional system, the solution of a matrix equation may be posed as an image-analysis problem. As we shall observe, discrete wavelet techniques may be suitable for the solution of large complex matrix equations.

Continuous techniques, on the other hand, may be suitable for time-domain processing, where the wavelet transform can be interpreted as a windowed Fourier transform. This we shall deal with in the second part of the paper.

3. Development of the discrete wavelet methodology from filter-theory concepts

3.1 Preliminaries

Consider the signal $x(t)$ that is discrete, so that it is represented by the sequence

$$x(n): n = 0,1,2,... \tag{1}$$

Then, its Fourier transform is best handled by the z transform (the lowercase letters are for functions in the original domain, and the uppercase letters are used for the z transform):

$$X(z) = X\left(e^{j2\pi f}\right) = X\left(e^{j\omega}\right) = \sum_n x(n) z^{-n}, \tag{2}$$

where $\omega = 2\pi f$ is the angular frequency, and $z = e^{j\omega} = e^{j2\pi f}$ Consider the sampled signal $x(n)$ to be bandlimited, and assume it is sampled (say) at $f = 1$Hz. Thus, the sampling interval is $\Delta t = 1$ sec. From the Nyquist sampling criterion, it is then necessary for the signal $x(n)$ to be bandlimited to 1/2 Hz, so that it can be sampled at two times its bandwidth at the Nyquist frequency without aliasing. The bandwidth of the signal (in angular frequency), ω_{band}, is

$$\omega_{band} = 2\pi f_{band} = 2\pi \cdot 1/2 = \pi, \tag{3}$$

and the sampling angular frequency, ω_{samp}, is

$$\omega_{samp} = 2\pi. \tag{4}$$

Now, let us filter the signal $x(n)$ by a low-pass filter, $H(z)$, of bandwidth $\pi/2$ [i.e., $0 \le \omega \le \pi/2$], and by a high-pass filter, $G(z)$, of bandwidth $\omega = \pi/2$ to π. Let $u'(n)$ be the low-pass-filtered signal [i.e., $u'(n)$ has been obtained by passing $x(n)$ through the low-pass filter $h(n)$], and let $v'(n)$ be the high-pass-filtered signal [i.e., $v'(n)$ has been obtained by passing $x(n)$ through the high-pass filter $g(n)$]. This is shown in Figure 1. Now, since the bandwidth of the signals $u'(n)$ and $v'(n)$ has been reduced by a factor

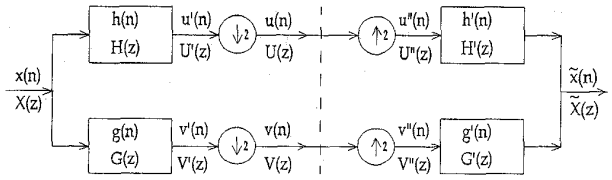

Figure 1. The principles of sub-band filtering.

of two, these signals can be decimated by a factor of two without any aliasing. This is equivalent to reducing the sampling rate. Decimation or down-sampling by a factor of two implies that alternate samples are dropped, and the data are compressed, as shown in Appendix 1 (Section 8). The purpose of decimation is to reduce the sampling rate and, thereby, the bandwidth of the signal. This down-sampling is possible because $u'(n)$ and $v'(n)$ have an effective bandwidth of $f = 1/4$ or $\omega = \pi/2$, because they have been filtered.

Next, both $u'(n)$ and $v'(n)$ are down-sampled by a factor of two, resulting in $u(n)$ and $v(n)$. This sub-sampling can continue further, as we shall see later on. Here, we will restrict ourselves to the two stages of filtering of $x(n)$ by $h(n)$ and $g(n)$, for illustration purposes. Since both $u(n)$ and $v(n)$ have a smaller bandwidth, they can be easily sampled, quantized, coded, and transmitted. In the receiver, the quantized, sampled, and coded $u(n)$ and $v(n)$ are received. The down-sampled versions, $u(n)$ and $v(n)$, can be transmitted at a much lower bit rate than the original signal, without any loss of information, as they have a smaller bandwidth than the original signal. The problem is how to reconstruct the signal $x(n)$ back again, given the sub-sampled versions $u(n)$ and $v(n)$ of $x(n)$, without any aliasing or distortion.

Using this type of sub-band splitting has many advantages:

1. This methodology results in a "maximally decimated" signal (i.e., some of the sample values of the signal have been deleted or set to zero), namely, the sampling rate can be reduced, without any loss of information. [Note that $v(n)$ of $x(n)$ have a lower bandwidth than the original signal $x(n)$ and, hence, the sample rate has been reduced by a factor of two]. This is equivalent to saying that $u(n)$ and $v(n)$ have been decimated by a factor of two.

2. Even if $u(n)$ and $v(n)$ are quantized in a very rough fashion (say, quantized into two bits, rather than the conventional eight bits or 16 bits), then the reconstruction is really remarkable, even though such large quantization errors are introduced in the coding of $u(n)$ and $v(n)$ [3-8]. This has been shown, at least in the area of image processing. We will also demonstrate that this happens in the compression of matrices arising in electromagnetic-field problems. Our interest in this is due to the fact that a matrix is essentially a discretized version of an image. So, can we apply this methodology to the efficient solution of operator equations? We will address this issue later on.

3. Mother Nature, in many cases, performs processing in such a way. For example, human ears and eyes, at least in the first stage of decoding sound and sight, perform processing by constant-Q filters that are very closely related to wavelets.

Next, the signal is reconstructed from the decimated transmitted signals $u(n)$ and $v(n)$. The signals are up-sampled by a factor of two to produce $u''(n)$ and $v''(n)$. The principle of up-sampling is shown in Appendix 2 (Section 9). Then, they are filtered by two receiving filters, $g'(n)$ and $h'(n)$. The outputs are combined to form $\tilde{x}(n)$. Now, let us see how $x(n)$ is related to its estimate $\tilde{x}(n)$, and then the methodology to extract $x(n)$ will be obvious.

Please observe that

$$U'(z) = H(z)X(z), \tag{5}$$

$$V'(z) = G(z)X(z). \tag{6}$$

From Appendix 1 (since $u(n)$ and $v(n)$ have been decimated by a factor of two)

$$U(z) = \frac{1}{2}\left[U'\left(\sqrt{z}\right) + U'\left(-\sqrt{z}\right)\right], \tag{7}$$

$$V(z) = \frac{1}{2}\left[V'\left(\sqrt{z}\right) + V'\left(-\sqrt{z}\right)\right]. \tag{8}$$

By using the results of Appendix 2 (where $u''(n)$ and $v''(n)$ have been up-sampled by a factor of two),

$$U''(z) = U\left(z^2\right) = \frac{1}{2}\left[U'(z) + U'(-z)\right], \tag{9}$$

$$V''(z) = V\left(z^2\right) = \frac{1}{2}\left[V'(z) + V'(-z)\right]. \tag{10}$$

Therefore,

$$\begin{aligned}\tilde{X}(z) &= \frac{1}{2}\{\left[G(z)X(z) + G(-z)X(-z)\right]G'(z) \\ &\quad + \left[H(z)X(z) + H(-z)X(-z)\right]H'(z)\}\end{aligned} \tag{11}$$

$$\begin{aligned}&= \frac{1}{2}\{\left[G(z)G'(z) + H(z)H'(z)\right]X(z) \\ &\quad + \left[G(-z)G'(z) + H(-z)H'(z)\right]X(-z)\},\end{aligned} \tag{12}$$

where $\tilde{X}(z)$, $G'(z)$, $H'(z)$, $G(z)$, $H(z)$, and $X(z)$ are the z transforms of $\tilde{x}(n)$, $g'(n)$, $h'(n)$, $g(n)$, $h(n)$, and $x(n)$. The z transform has been defined by Equation (2).

The estimated signal $\tilde{X}(z)$ contains the original signal (which is given by the first term) and an aliased part (which is given by the second term of Equation (12)). Now, to remove the aliasing effect, the second term must be zero, i.e.,

$$H(-z)H'(z) + G(-z)G'(z) = 0. \tag{13}$$

Let $H(z)$ be a FIR (finite-impulse-response) filter of order $N+1$. Then, $h(n)$ will have $N+1$ terms. We consider N to always be odd. Then,

$$H(z) = h(0) + h(1)z^{-1} + \ldots + h(N)z^{-N}. \tag{14}$$

Without loss of generality and for convenience we choose

$$H'(z) = z^{-N}H\left(z^{-1}\right) \text{ so that } h'(n) = h(N-n). \tag{15}$$

The factor z^{-N} is used to guarantee causality of the filters [i.e., $h'(n) = 0$ for $n < 0$]. The high-pass filter $g'(n)$ is chosen in such a way that

$$G'(z) = z^{-N}G\left(z^{-1}\right) \text{ with } g'(n) = g(N-n). \tag{16}$$

In addition, we define the high-pass filter $g'(n)$ in terms of the low-pass filter coefficients $h'(n)$ by choosing

$$\begin{aligned}g'(n) &= -(-1)^n h'(N-n) = -(-1)^n h(n), \\ g(n) &= (-1)^n h(N-n) = (-1)^n h'(n),\end{aligned} \tag{17}$$

so that

$$\begin{aligned}G'(z) &= z^{-N}H'\left(-z^{-1}\right) = -H(-z), \\ G(z) &= -z^{-N}H\left(-z^{-1}\right) = H'(-z).\end{aligned} \tag{18}$$

Substitution of Equations (18) into Equation (13) demonstrates that all four equations are consistent, and the aliased component due to $X(-z)$ is zero.

Furthermore, by utilizing Equations (15) and (16), Equation (12) simplifies to

$$\begin{aligned}\tilde{X}(z) &= \frac{1}{2}\left[z^{-N}G(z)G\left(z^{-1}\right) + z^{-N}H(z)H\left(z^{-1}\right)\right]X(z) \\ &= \frac{1}{2}\left[H\left(-z^{-1}\right)H(-z) + H(z)H\left(z^{-1}\right)\right]z^{-N}X(z).\end{aligned} \tag{19}$$

If the filter $H(z)$ is chosen in such a way that

$$H(-z)H\left(-z^{-1}\right) + H(z)H\left(z^{-1}\right) = 2, \tag{20}$$

or

$$\left|H\left(e^{j\omega}\right)\right|^2 + \left|H\left[e^{j(\omega+\pi)}\right]\right|^2 = 2, \tag{21}$$

then one would have a perfect reconstruction property:

$$\tilde{X}(z) = z^{-N}X(z); \qquad \tilde{x}(n) = x(n-N); \tag{22}$$

and the estimated signal is delayed by N samples.

The filters $H(z)$ and $G(z)$ are called quadrature mirror filters (QMF), because they have symmetry around the point $\pi/2$, as shown in Figure 2. Ideally, we would prefer $H(z)$ and $G(z)$ to be

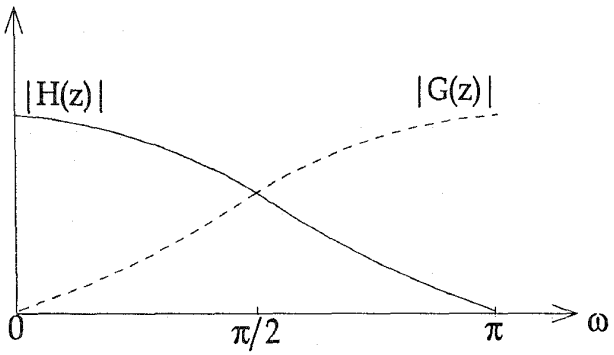

Figure 2. The quadrature mirror filters.

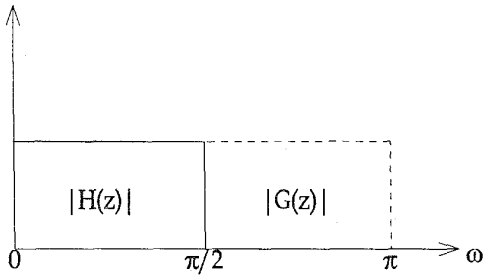

Figure 3. Non-overlapping ideal filters.

non-overlapping, as shown in Figure 3. However, due to realizability conditions, they are like those presented in Figure 2. Moreover, we would like to have $H(z)$ and $G(z)$ be FIR filters (finite impulse response), as opposed to IIR (infinite impulse response), for ease of numerical computation. To illustrate the nature of the various FIR filters given by the various equations, consider as an example $N=3$ [9]. Then, the various filters $H(z)$, $G(z)$, $H'(z)$, and $G'(z)$ will have four nonzero coefficients in their expansion. Or, equivalently, $h(n)$, $g(n)$, $h'(n)$, and $g'(n)$ will have four entries. They will have the following form. If we choose

$$H(z)=\sum_{n=0}^{N}h(n)z^{-n}=h(0)+h(1)z^{-1}+h(2)z^{-2}+h(3)z^{-3}, \quad (23)$$

then from Equation (18),

$$\begin{aligned}G(z)&=-z^{-3}H\left(-z^{-1}\right)\\&=-z^{-3}\left[h(0)-h(1)z^{+1}+h(2)z^{+2}-h(3)z^{+3}\right]\\&=+h(3)-h(2)z^{-1}+h(1)z^{-2}-h(0)z^{-3},\end{aligned} \quad (24)$$

and from Equation (15),

$$\begin{aligned}H'(z)&=z^{-N}H\left(z^{-1}\right)\\&=h(3)+h(2)z^{-1}+h(1)z^{-2}+h(0)z^{-3},\end{aligned} \quad (25)$$

and finally from Equation (18),

$$\begin{aligned}G'(z)&=z^{-N}G\left(z^{-1}\right)=-H(-z)\\&=-h(0)+h(1)z^{-1}-h(2)z^{-2}+h(3)z^{-3}.\end{aligned} \quad (26)$$

So, if we solve only for $H(z)$, the other three filters of Figure 1 will then be given by Equations (24), (25), and (26).

Now, we show how to solve for $H(z)$. In this example, we have $N=3$, and the order of the filter, L, is given by

$$L=\text{order of filter}=N+1=4. \quad (27)$$

Utilizing Equation (20), we have

$$\begin{aligned}&\left[h(0)-h(1)z^{-1}+h(2)z^{-2}-h(3)z^{-3}\right]\\&\quad\times\left[h(0)-h(1)z+h(2)z^{2}-h(3)z^{3}\right]\\&+\left[h(0)+h(1)z^{-1}+h(2)z^{-2}+h(3)z^{-3}\right]\\&\quad\times\left[h(0)+h(1)z+h(2)z^{2}+h(3)z^{3}\right]=2.\end{aligned} \quad (28)$$

Equating all the coefficients related to the individual powers of z in Equation (28) leads to

$$h^2(0)+h^2(1)+h^2(2)+h^2(3)=1 \quad (\text{for } z^0), \quad (29)$$

$$h(0)h(2)+h(1)h(3)=0 \quad (\text{for } z^2 \text{ and } z^{-2}). \quad (30)$$

We need two more equations to solve for $H(z)$. Since $G(z)$ is a high-pass filter, then at $\omega=0$,

$$G\left(e^{j0}\right)=G(1)=0=H\left(e^{j\pi}\right)=H(-1). \quad (31)$$

From Equation (23), this leads to

$$-h(3)+h(2)-h(1)+h(0)=0. \quad (32)$$

In addition, from Equations (21) and (31) at $\omega=0$ we have

$$H(1)=H\left(e^{j0}\right)=\sqrt{2}. \quad (33)$$

From Equations (23) and (33) we get

$$H\left(e^{j0}\right)=H(1)=h(0)+h(1)+h(2)+h(3)=\sqrt{2}. \quad (34)$$

From Equations (32) and (34) we see that

$$h(0)+h(2)=\frac{1}{\sqrt{2}}, \quad (35)$$

$$h(1)+h(3)=\frac{1}{\sqrt{2}}. \quad (36)$$

In addition one has Equations (29) and (30). We need one more equation, as these four equations [Equations (29), (30), (35), and (36)] are linearly dependent, since Equations (35) and (36), in conjunction with Equation (30), lead to Equation (29). The question is how to find the fourth equation. Without the fourth equation it is not possible to get the complete solution. Here, the various methodologies differ, and different researchers have come up with different procedures.

For example, Daubechies [1] originally developed this methodology by constraining the filter $H(z)$ to be smooth, by enforcing all derivatives to be zero at $\omega = 0$, up to order p, or, equivalently, $G'^{p}(1) = 0$, where the superscript p denotes the pth derivative of G'. The actual value for p is determined from the number of equations needed to solve for the values of $h(n)$, $n = 0,1,\ldots,N$. This leads to taking the various moments of $g'(n)$ and setting them equal to zero. Daubechies chose this procedure because enforcing the above conditions guarantees smooth wavelets, which we will define later. However, for the present case, where the number of discrete wavelet coefficients is finite, the smoothness of the wavelets is a moot point. This is true since for the discrete case, the wavelet transform can be implemented (for the examples that we are interested in) without explicitly specifying the wavelets. The smoothness of the wavelets at this point, then, is of no concern to us! Another approach, for example, is given in [10, 11].

In mathematical terms, setting the derivative of $G'(1)$ to zero leads to

$$-0h(0) - 1h(1) + 2h(2) - 3h(3) = 0. \tag{37}$$

Solution of Equations (30), (35), (36), and (37) leads to

$$\begin{aligned} h'(0) = h(3) &= \frac{1+\sqrt{3}}{4\sqrt{2}}, \\ h'(1) = h(2) &= \frac{3+\sqrt{3}}{4\sqrt{2}}, \\ h'(2) = h(1) &= \frac{3-\sqrt{3}}{4\sqrt{2}}, \\ h'(3) = h(0) &= \frac{1-\sqrt{3}}{4\sqrt{2}}. \end{aligned} \tag{38}$$

The magnitude and the phase responses of $H(z)$, $H'(z)$, $G(z)$, $G'(z)$ are shown in Figures 4a and 4b, respectively. Note that these filters have no ripples, with many zeros at π. The slope at the center is proportional to $\sqrt{N}$. The transition from $|H(z)| = 0.98\sqrt{2}$ to $|H(z)| = 0.02\sqrt{2}$ is over an interval of length $4/\sqrt{N}$.

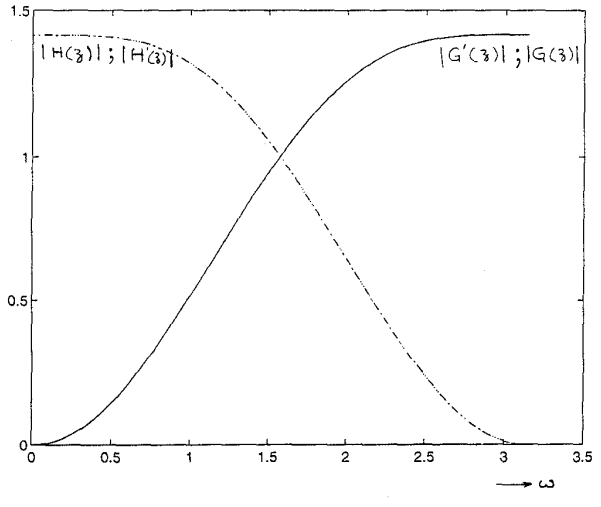

Figure 4a. The magnitude responses of the fourth-order filters.

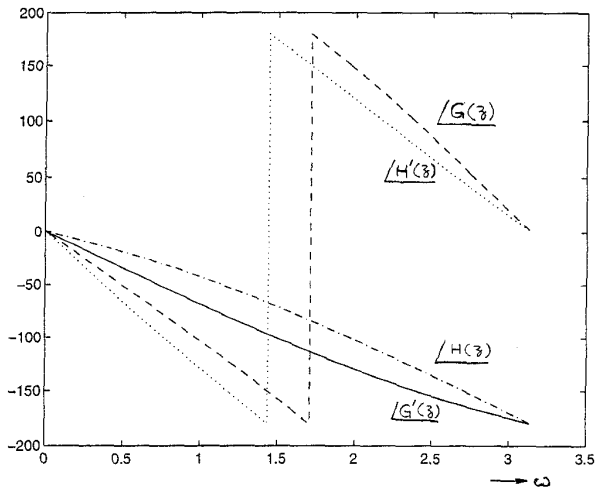

Figure 4b. The phase responses of the fourth-order filters.

Instead of having a two-stage decomposition of the signal $x(n)$ into $u'(n)$ and $v'(n)$, one can perform a multistage decomposition by applying the filters successively to each stage of the decomposition, as shown in Figure 5. The electrical-filter-theory equivalent is shown in Figure 6. This is the decomposition part (or the part labeled "transmitter" in Figure 1). The coefficients at the output of Figure 5 are then thresholded. This is equivalent to keeping only those coefficients that are bigger in magnitude than some constant ε. The values smaller than ε are set equal to zero, resulting in the approximate filter output. Now, the interesting part is that these "filtered" thresholded coefficients can now be used to recover the original signal with an accuracy better than ε (!). (We will see this feature later on). The reconstruction algorithm is depicted in Figure 7, where the approximated coefficients are upsampled, and then filtered the way that is depicted in the receiver of Figure 1.

The type of decomposition outlined in Figure 5 is identical to a wavelet decomposition, as the next section will illustrate. For example, filtering a function by $h(n)$ is equivalent to fitting a scaling function at a certain scale, and filtering by $g(n)$ is equivalent to curve fitting $x(n)$ by wavelets at the same scale as the scaling function. The mathematical connection is now established between wavelet theory and filter theory.

3.2 Connection between the filter theory and the mathematical theory of wavelets

To establish a connection between the filter theory and the mathematical theory of wavelets, we will deal with functions of a real continuous variable. Discrete samples then will be viewed as a "sample and hold" of the these functions of a continuous variable. Such an approach is absolutely necessary, because the wavelets cannot be expressed in terms of discrete samples. Moreover, the dilation equation, which is at the heart of wavelet theory, has no solutions for the discrete samples. So, the discrete wavelet transform implies that the functions we are dealing with are functions of

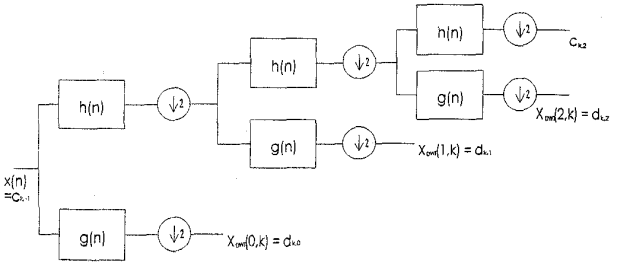

Figure 5. A multistage decomposition of the signal $x(n)$.

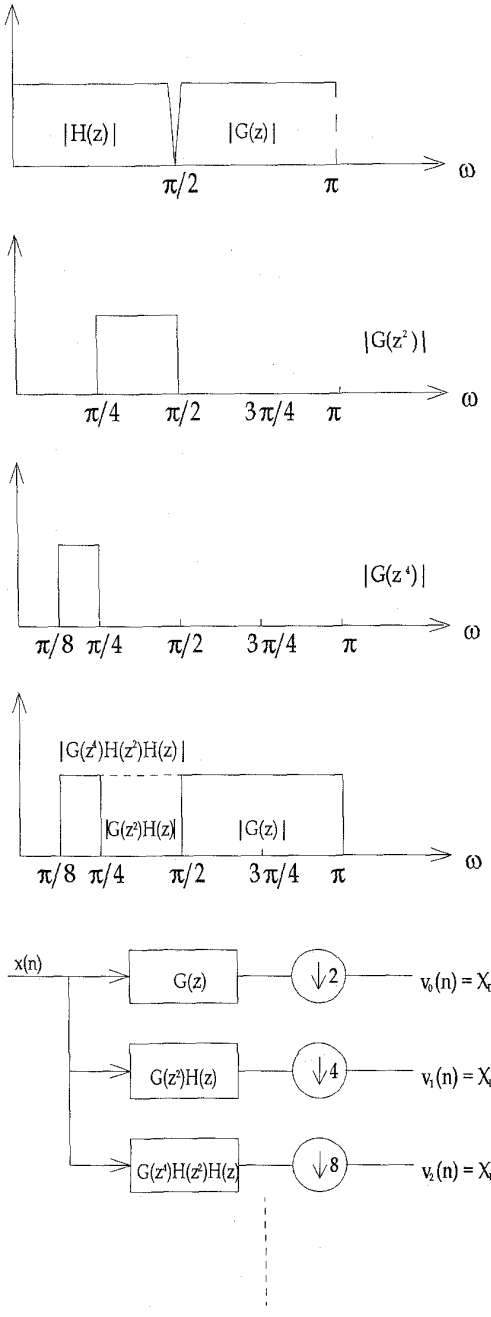

Figure 6. A filter-theory representation of the discrete wavelet transform.

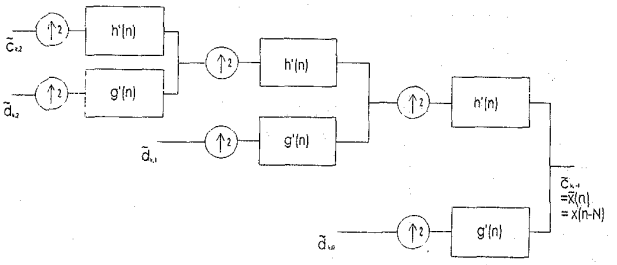

Figure 7. The reconstruction of the original signal, $x(n)$, from the approximate coefficients of the discrete wavelet transform.

a continuous variable. They can have integer shifts. In addition, they can be scaled up and down by integer multiples.

We consider the original signal, $x(t)$, with bandwidth from 0 to π. Also, consider some functions $\phi(t)$. We assume that the integer shifts m of $\phi(t)$, namely $\phi(t-m)$, are a Riesz basis for the original space [38]. Let us denote

$$\phi_m(t) = \phi(t-m). \tag{39}$$

Hence, one can represent a dilated version of $\phi(t)$–namely, $\phi(t/2)$–by a combination of the functions $\phi(t-m)$ [or $\phi_m(t)$] with some coefficients $h'(m)$, resulting in the dilation equation

$$\phi\left(\frac{t}{2}\right) = \sqrt{2}\sum_{m=0}^{N} h'(m)\phi(t-m), \tag{40}$$

or, equivalently, [with $h'(n) = h(N-m)$, as defined by Equation (15)]

$$\phi(t) = \sqrt{2}\sum_{m=0}^{N} h'(m)\phi(2t-m) = \sqrt{2}\sum_{m=0}^{N} h(N-m)\phi(2t-m). \tag{41}$$

It is interesting to note that the coefficients $h'(m)$ turn out to be the same coefficients that we have described earlier in the receiver part of Figure 1 and Figure 7.

As an example, consider $\phi(t)$ to be a pulse function of magnitude 1, located between 0 and 1, as shown in Figure 8. Then, $\phi(t/2)$ has support from 0 to 2, or is a dilated version of $\phi(t)$. Please note that $\phi(t)$ can be represented by $\phi(2t)$ and $\phi(2t-1)$, where each of these functions is defined between 0 to 1/2 and 1/2 to 1, respectively. In this case, $h'(0) = h'(1) = 1/\sqrt{2}$. Equation (41) essentially reflects the basis of the dilation equation: i.e., the function can be approximated by a weighted sum [through $h'(m)$] of the shifted and dilated versions of the same function.

The function $\phi(t)$, which solves the dilation equation for a particular $h'(m)$, is called the scaling function, and is also called the father of wavelets. Also, note that the functions $\phi(t-m)$ are assumed to be normalized, i.e.,

$$\int_t \phi(t-m)dt = 1. \tag{42}$$

Here, "dt"can be represented as the incremental interval length. Therefore, from Equation (41), utilizing Equation (42), we get

$$\int_t \phi(t-k)dt = 1 = \sqrt{2}\sum_{m=0}^{N} h'(m)\int_t \frac{\phi(2t-2k-m)}{2} d(2t) = \frac{\sqrt{2}}{2}\sum_{m=0}^{N} h'(m) \tag{43}$$

or, equivalently,

$$\sum_{m=0}^{N} h'(m) = \sqrt{2}\,. \tag{44}$$

Hence, the coefficients $h'(m)$, satisfying the dilation equation, must satisfy Equation (44). This is the same equation as Equation (34), restricted to $N=3$ terms. The corresponding wavelets are given by (compare with Equation (17))

$$\begin{aligned}\psi(t) &= \sqrt{2}\sum_{m=0}^{N} g'(m)\phi(2t-m) \\ &= \sqrt{2}\sum_{m=0}^{N} -(-1)^m h'(N-m)\phi(2t-m)\,,\end{aligned} \tag{45}$$

where $N+1$ is the order of the filter (which is always even). Here, the filter coefficients $h'(m)$ and $g'(m)$ have been assumed to be real. The function $\psi(t)$, for a given $g'(m)$, is called the mother of wavelets. (This might be viewed as the traditional Judeo Christian concept of mother: where the mother is generated from the father!)

So, from an electrical-engineering perspective, if we have the filter coefficients $h'(m)$, then the scaling function $\phi(t)$ can be obtained by iteratively solving the dilation Equation (41). This is carried out by starting with letting $\phi(t)$ be a pulse function, and then filtering by $h'(m)$, and continuing until convergence is reached. Once the scaling function is known, the wavelets are given by Equation (45).

The scaling function can also be solved for in the transform domain. By taking the Fourier transform of Equation (41), one can write the dilation equation in the ω domain as

$$\hat{\phi}(\omega) = \frac{\sqrt{2}}{2} H'\left(e^{-j\omega/2}\right)\hat{\phi}(\omega/2), \tag{46}$$

where $\hat{\phi}(\omega)$ is the Fourier transform of $\phi(t)$, and $H'(z)$ is the z transform of $h'(n)$ (see Equation (15)). One can repeatedly apply Equation (46) to obtain

$$\hat{\phi}(\omega) = \left[\prod_{k=1}^{n} 2^{-1/2} H'\left(e^{-j\omega/2^k}\right)\right]\hat{\phi}\left(\omega/2^n\right). \tag{47}$$

Owing to Equation (42), $\hat{\phi}(0)=1$. Therefore, in the limit $n\to\infty$, Equation (47) becomes

$$\hat{\phi}(\omega) = \left[\prod_{k=1}^{\infty} 2^{-1/2} H'\left(e^{-j\omega/2^k}\right)\right] = \prod_{k=1}^{\infty}\left[2^{-1/2} H'\left(e^{-j\omega/2^k}\right)\right] \tag{48}.$$

The solution for $\hat{\phi}(\omega)$ is point-wise convergent, provided the infinite series converges. In the original domain, this is equivalent to $\phi(t) = \prod_{k=1}^{\infty}\left[*2^{-1/2}h'\left(2^k t\right)\right]$, where $*$ denotes a convolution. Note that the sequence of convolutions is carried out by various compressed versions of the same signal. When the sequence of convolutions converges, it yields the function $\phi(t)$.

When $N=0$, the dilation equation becomes, for $h'_0=\sqrt{2}$,

$$\phi(t) = \phi(2t)\,,$$

and the scaling function becomes a delta function. If we choose $L=N+1=2$ and

$$h'_0 = \frac{1}{\sqrt{2}} = h'_1. \tag{49}$$

Hence, in this case, the dilation equation is $\phi(t)=\phi(2t)+\phi(2t-1)$. One possible solution of this dilation equation is the pulse function:

$$\phi(t) = \begin{cases} 1 \text{ if } 0 \le t < 1 \\ 0 \text{ otherwise} \end{cases}. \tag{50}$$

The wavelet is generated from Equation (45), and is given by

$$\psi(t) = \begin{cases} -1 \text{ for } 0 \le t < 1/2 \\ +1 \text{ for } 1/2 \le t < 1 \\ 0 \quad \text{otherwise} \end{cases}, \tag{51}$$

since $\psi(t)=-\phi(2t)+\phi(2t-1)$. This is shown in Figure 8. This is the pulse doublet, and it is related to the Haar wavelet. Please note that the scaling function $\phi(t)$ is in this case orthogonal with respect to its own translates, i.e.,

$$\int_{-\infty}^{\infty}\phi(t)\phi(t-m)dt = 0. \tag{52}$$

This is also true for the wavelets:

$$\int_{-\infty}^{\infty}\psi(t)\psi(t-m)dt = 0. \tag{53}$$

For $N=3$, we obtain the case presented earlier. Note that for this case, the filter coefficients h'_i are given by Equation (38). Hence,

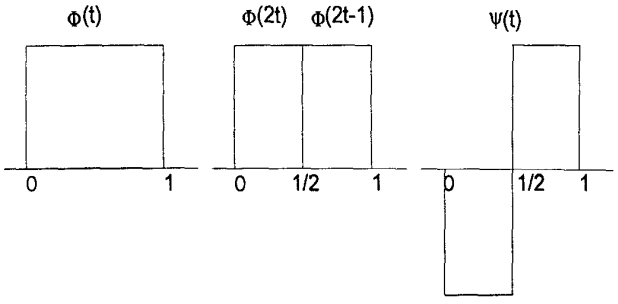

Figure 8. An example of the dilation equation for $M=2$.

the scaling function can be obtained from the solution of the dilation equation,

$$\phi(t)=\frac{1}{4}\left[\left(1+\sqrt{3}\right)\phi(2t)+\left(3+\sqrt{3}\right)\phi(2t-1)+\left(3-\sqrt{3}\right)\phi(2t-2)+\left(1-\sqrt{3}\right)\phi(2t-3)\right]. \quad (54a)$$

The wavelets are generated in an analogous fashion by using Equations (45) and (38), resulting in

$$\psi(t)=\frac{-1}{4}\left[\left(1-\sqrt{3}\right)\phi(2t)-\left(3-\sqrt{3}\right)\phi(2t-1)+\left(3+\sqrt{3}\right)\phi(2t-2)-\left(1+\sqrt{3}\right)\phi(2t-3)\right]. \quad (54b)$$

We are not going to delve further into the solution of the dilation equation, since for the discrete wavelet transform and for the problems that we are interested in electromagnetics–namely, solutions of large matrix equations–the scaling functions and the wavelets are really not necessary. This is because the discrete wavelet representation can be carried out from the knowledge of only $h(m)$! However, we present some other wavelets for illustration purposes.

For example, consider the Shannon wavelet, which is the dual of the Haar wavelet. The scaling function is given by

$$\phi(t)=\frac{\sin \pi t}{\pi t},$$

and its transform is given by

$$\hat{\phi}(\omega)=\begin{cases}1 & \text{for } 0\le|\omega|<\pi\\ 0 & \text{otherwise}\end{cases}.$$

The wavelet can be generated from Equation (45), and is given by

$$\psi(t)=\frac{\sin \pi t}{\pi t}\cos\frac{3\pi t}{2},$$

and its transform is

$$\hat{\psi}(t)=\begin{cases}1 & \text{for } \pi<|\omega|<2\pi\\ 0 & \text{otherwise}\end{cases}.$$

Lagrange half-band filters are used when one needs a non-negative frequency response of the filters $h(n)$. A closed-form expression was given by Ansari [12], starting from

$$H'(z)=\frac{1}{2}+\sum_{n=1}^{i}h_i'(2n-1)\left[z^{-2n+1}+z^{2n-1}\right],$$

with $4i-1$ coefficients. The coefficients h_i' are determined using the Lagrange interpolation formula:

$$h_i'(2n-1)=\frac{(-1)^{n+i-1}\prod_{k=1}^{2i}(i-k+1/2)}{(i-n)!(i-1+n)!(2n-1)}.$$

These filters are very regular, as they have a $2i$-fold zero at $z=-1$.

The confusing part here is what to use as the starting point for a scientific endeavor to carry out a numerical analysis utilizing wavelets? There are two choices:

1. Do we start with $\phi(t)$, construct $h'(n)$, and then generate $\psi(t)$ [from Equation (45)]?; or

2. Do we start with $h'(n)$, and then create $\phi(t)$ and $\psi(t)$?

For the discrete case that we are dealing with, the answer is straightforward: that is, we design $h'(n)$, and then obtain $\phi(t)$ and $\psi(t)$. This is also much simpler in practice. However, for the discrete wavelet transform, as we shall see, $\phi(t)$ and $\psi(t)$ are not at all required in the numerical computation!

In summary, the mathematical basis of the wavelets has been presented from a filter-theory perspective. How to construct scaling functions ϕ and wavelets ψ has been shown, starting from the filters $h'(m)$, and utilizing the perfect-reconstruction argument presented with subband-filtering techniques. Once $h'(m)$ is known, ϕ can be generated from Equation (41), and ψ, from Equation (45).

4. Approximation of a function by wavelets

Consider a function $x(t)$. The objective is to approximate it by the wavelets $\psi_{n,k}(t)$, i.e.,

$$x(t)=\sum_{n=-\infty}^{\infty}\sum_{k=-\infty}^{\infty}d_{k,n}\psi_{n,k}(t), \quad (55)$$

where we define the wavelets by

$$\psi_{n,k}(t)=2^{-n/2}\psi\left(2^{-n}t-k\right). \quad (56)$$

Note that $\psi\left(2^{-n}t\right)$ represents a dilated version of $\psi(t)$. For $n=-1$, we say the scale is the finest. This is because for $n>-1$, the function gets dilated and becomes wider. $\psi(t-k)$ represents the shifts. Therefore, we approximate the function $x(t)$ by a dilated and shifted version of the same function $\psi(t)$. We assume that we are dealing with orthogonal wavelets, hence

$$\int\psi_{j,k}(t)\psi_{n,i}(t)dt=0 \text{ if } j\ne n \text{ or } k\ne i. \quad (57)$$

The scale factor $2^{-n/2}$, appearing in Equation (56), is there so as to make the functions $\psi_{n,k}(t)$ orthonormal, i.e.,

$$\int\psi_{j,k}(t)\psi_{n,i}(t)dt=\delta_{jn}\delta_{ki}. \quad (58)$$

It is interesting to note that $\psi_{n,k}(t)$ has zero DC value ($\psi_{n,k}(\omega=0)=0$, whereas $x(t)$ may not! Therefore, if we have to talk about convergence of the series in Equation (55), we can only talk about mean-square convergence. This dichotomy, however, does not arise when the sum in Equation (55) is finite. Utilizing Equations (58) and (55), we observe that

$$d_{k,n} = \int x(t)\psi_{n,k}(t)dt = \langle x;\psi_{n,k}\rangle = X_{DWT}(n,k), \qquad (59)$$

and these are the discrete wavelet coefficients of the function $x(t)$. These are the same values shown in Figure 5. Our objective in this section is to establish that isomorphism.

Now, if we have to carry out the inner products in Equation (59), it will be extremely time consuming, as the inner products have to be carried out for all values of n and k. Here, the strength of the wavelet techniques comes in, as they provide a fast and accurate way to recursively evaluate the inner products. This is accomplished through the introduction of the scaling functions

$$\phi_{i,j}(t) = 2^{-i/2}\phi\left(2^{-i}t - j\right). \qquad (60)$$

We further assume/utilize the orthogonality relationships between the scaling functions and the wavelets, and between the scaling functions themselves, i.e.,

$$\int \phi_{j,k}(t)\psi_{i,n}(t)dt = 0 \text{ if } i \le j, \qquad (61)$$

and

$$\int \phi_{j,k}(t)\phi_{j,n}(t)dt = \delta_{k,n}. \qquad (62)$$

We now define the coefficients $c_{k,n}$ through

$$c_{k,n} = \int x(t)\phi_{n,k}(t)dt. \qquad (63)$$

It is now shown how the $d_{k,n}$ are evaluated recursively through the $c_{k,n}$.

We have, from Equations (58), (61), and (62), that the following orthonormal set

$$\{\phi(t-k);\psi(t-k)\}_{k=-\infty}^{\infty} \qquad (64)$$

represents a basis, as the functions involved in the set are orthogonal. From the dilation equation, Equation (41), and from Equation (45), we note that

$$\{\sqrt{2}\phi(2t-k)\}_{k=-\infty}^{\infty}$$

also form an orthonormal set for the same space. This is for scale $n=-1$, as defined by Equation (56). Therefore, we can expand any function $p(t)$ by

$$p(t) = \sum_k a^{(-1)}(k)\sqrt{2}\phi(2t-k) \qquad (65a)$$

$$= \sum_k \left[a^0(k)\phi(t-k) + b^0(k)\psi(t-k)\right]. \qquad (65b)$$

Here, $a^{(-1)}(k)$ are the coefficients used to represent the function $p(t)$ by $\phi(2t-k)$. The superscripts j on the coefficients $a^j(k)$ and $b^j(k)$ represent the value of the scale j at which they are represented. We have from Equation (41),

$$\phi(t-n) = \sqrt{2}\sum_k h'(k)\phi(2t-2n-k), \qquad (66)$$

and from Equation (45),

$$\psi(t-n) = \sqrt{2}\sum_k g'(k)\phi(2t-2n-k). \qquad (67)$$

It is interesting to note that a byproduct of Equations (66) and (67) is that

$$\langle \phi_{0,k};\phi_{-1,j}\rangle = h'(j-2k)$$

$$\langle \psi_{0,k};\phi_{-1,j}\rangle = g'(j-2k),$$

which can be generalized to

$$\langle \phi_{n,k};\phi_{n-1,j}\rangle = h'(j-2k)$$

$$\langle \psi_{n,k};\phi_{n-1,j}\rangle = g'(j-2k).$$

Next, observe that

$$a^0(n) = \int_{-\infty}^{\infty} p(t)\phi(t-n)dt = \int_{-\infty}^{\infty} p(t)\sum_k h'(t)\sqrt{2}\phi(2t-2n-k)dt$$
$$= \sum_k h'(k)a^{(-1)}(2n+k) = \sum_k a^{(-1)}(k)h'(k-2n), \qquad (68)$$

and

$$b^0(n) = \sum_k a^{(-1)}(k)g'(k-2n). \qquad (69)$$

Given the existence of relationships like Equations (68) and (69), and drawing the isomorphism between

$$c_{k,j} \leftrightarrow a^j(k),$$

$$d_{k,j} \leftrightarrow b^j(k),$$

we can generalize the expressions of Equations (68) and (69) to

$$c_{k,j+1} = \sum_n c_{n,j}h'(n-2k) = \sum_n c_{n,j}h(N+2k-n) \text{ for } j \ge -1, \qquad (70a)$$

$$d_{k,j+1} = \sum_n c_{n,j}g'(n-2k) = \sum_n c_{n,j}g(N+2k-n) \text{ for } j \ge -1. \qquad (70b)$$

These results have been derived utilizing Equations (15) and (16). The above recursive relations show that we need to compute the inner product of Equation (63) at the highest scale, $n=-1$, only once (instead of using Equation (59)), and then the wavelet coefficients $d_{k,n}$ of the $X_{DWT}(n,k)$ ($n=0,1,2,\ldots$) are computed recursively from Equations (70a) and (70b). From a filter-theory point of view, Equations (70a) and (70b) show that the $c_{n,j}$ need to be convolved with $h(n)$ and $g(n)$, then down-sampled by a factor of two. Through Figure 5 and from the above development, it is clear that for the computation of the discrete wavelet transform (DWT),

it is not necessary to even know what the scaling functions and wavelets are, as one can directly use Equations (70a) and (70b) without going through the mathematical derivations, as Figures 5 and 6 illustrate. One starts with $c_{n,-1}$, which is the coefficient generated by correlating $\phi(2t)$ with the function $x(t)$, and then recursively computes the discrete wavelet transform mathematically through Equations (70a) and (70b), and graphically using Figure 5, which is easier to visualize from a filter-theory perspective. The methodology is the same. The process described so far is similar to the transmitter part as labeled in Figure 1. If the $\phi(2t)$ are the impulse scaling functions, then $c_{k,-1}$ will be equivalent to the sampled version of $x(t)$, namely $x(n)$.

There is another subtle point that one should introduce now! So far, in the approximation in Equation (55), the limits are infinity. This is good from a mathematical perspective. However, from a practical reality, the limits have to be finite. Hence, in addition to $d_{k,n}$, we also have $c_{k,n}$. The approximation of $x(t)$ from a practical standpoint is done by

$$x(t) = \sum_{n=0}^{M} \sum_{k} d_{k,n} \psi_{n,k}(t) + \sum_{k} c_{k,M} \phi_{M,k}(t). \qquad (71)$$

Hence, we have both wavelets and scaling functions in the approximation. This very important feature is generally not clearly delineated in many presentations. Now, observe that Equation (71) is the representation of $x(t)$.

In summary, the evaluation of the discrete wavelet coefficients in Equation (55) is equivalent to filtering the coefficient $c_{k,-1}$ obtained from $x(t)$ (or, equivalently, the sampled values of $x(t)$ for a certain class of scaling functions) by a cascade of mutually orthogonal filters, as shown in Figure 5. The bandwidth of the filters is reduced by a factor of two as one goes towards the DC value. For the infinite sum in Equation (55), the scaling function does not enter into the final sum, except in the intermediate computations. However, if the sum is finite in Equation (55), then one obtains Equation (71), and the scaling functions are needed in the summation.

Figure 9a. The original picture of "Lena."

Figure 9b. A compressed version of the picture of "Lena," utilizing QMF compression (40:1 compression).

Figure 9c. A compressed version of the picture of "Lena," utilizing JPEG compression (40:1 compression).

In practice, once the coefficients $d_{k,n}$ and $c_{k,m}$ have been obtained, those coefficients with magnitudes below a certain threshold value of ε (e.g., $\varepsilon = 10^{-3}$) are set equal to zero. At this point, the transmitter then sends out the approximate coefficients $\tilde{d}_{k,n}$ and $\tilde{c}_{k,M}$, which are the values obtained after thresholding $d_{k,n}$ and $c_{k,m}$ by ε. Now the problem is, how does one recover $x(t)$ from these approximate coefficients in a fast efficient way?

By utilizing Equations (66) and (67) in Equation (65b), we get

$$p(t)=\sum_k\left[a^{(0)}(k)\sqrt{2}\sum_n h'(n)\phi(2t-2k-n)+b^{(0)}(k)\sqrt{2}\sum_n g'(n)\phi(2t-2k-n)\right] \tag{72}$$

$$=\sum_k\sqrt{2}\left[a^{(0)}(k)\sum_n h'(n-2k)\phi(2t-n)+b^{(0)}(k)\sum_n g'(n-2k)\phi(2t-n)\right].$$

By equating Equation (72) to Equation (65a), we find

$$a^{(-1)}(k)=\sum_n\left[h'(k-2n)a^{(0)}(n)+g'(k-2n)b^{(0)}(n)\right] \tag{73}$$

$$=\sum_n\left[h(N+2n-k)a^{(0)}(n)+g(N+2n-k)b^{(0)}(n)\right].$$

Hence, we start with the approximate coefficients $\tilde{c}_{k,M}$ and $\tilde{d}_{k,n}$, and we then recursively generate, through the use of a generalization of Equation (73), the coefficients

$$\tilde{c}_{k,m-1}=\sum_n\left[h(N+2n-k)\tilde{c}_{n,m}+g(N+2n-k)\tilde{d}_{n,m}\right]. \tag{74}$$

Note that the $\tilde{c}_{k,-1}$ are the estimates of the discrete values of $x(n)$ for the impulse scaling functions. Also, observe that Equation (74) is equivalent to Figure 7, from a filter-theory perspective, and is identical to the receiver point in Figure 1. The most remarkable point here is that even though the original coefficients have been thresholded by ε to produce the approximate coefficients, $\tilde{c}_{k,M}$ and $\tilde{d}_{k,n}$, the original sampled function $x(n)$ can be reconstructed through $\tilde{x}(n)$ with an accuracy better than ε. This we will illustrate through numerical examples in the next section.

In summary, in order to implement and carry out the discrete wavelet transform, it is not even necessary to introduce the concept of scaling functions and wavelets. The filter-theory approach essentially provides the same methodology, in a simpler, practical fashion.

As an illustration of how to utilize the discrete wavelet transform, we consider the compression of an image. For the case of images, one is dealing with the two-dimensional discrete wavelet transform, which is a generalization of the one-dimensional case.

In the following examples, we consider the image to be a two-dimensional array. We take the discrete wavelet transform in two dimensions by utilizing a recursive relationship similar to Equations (70a) and (70b). We utilize an eighth-order filter that has been designed to match the signal [21]. Once the discrete wavelet coefficients are obtained, they are thresholded, and then the original image is reconstructed utilizing the recursive relation of Equation (74). The objective is to illustrate that even though only a few bits are utilized to code the compressed image, the reconstruction is still better than the conventional JPEG algorithm [21].

As an example, consider the original image of "Lena," shown in Figure 9a. The images in Figures 9b and 9c show the result of a 40:1 compression of "Lena," using wavelet techniques utilizing both signal-dependent QMF filters and JPEG compression. (JPEG is the current standard for image compression, and the coefficients of the filters $h(m)$ are determined from the signal). Here, compression refers to the total number of bits required to store the image, as opposed to the total number of bits of the original image. Even though there is noticeable degradation in both of the images, the two methods perform reasonably in the reconstruction of the image. This is due to the fact that the image is compressed by blocks. The image compressed utilizing the signal-dependent QMF decomposition looses detail in the local (i.e., high-frequency) edge information. In particular, notice that the sharpness in the eyes and the detail in the feather cap are blurred. Unlike the JPEG-compressed image, however, there are no objectionable artifacts, such as the "blockiness" mentioned earlier.

As another example, consider the application to halftone images. Unlike continuous-tone images, such as photographs, a halftone image is digital in nature: all pixels are either on or off. These digital pixels are densely placed on the paper (as many as 2400 per inch, to emulate high-quality magazine halftones). Halftone images are produced by photographing a continuous-tone image through a very fine screen, typically having 100-133 lines per inch. They are also often simulated–with lower resolution and quality–on common digital printers, including laser, ink-jet, and dot-matrix printers. It has become common for such images to be scanned into a computer using an 8-30 bits/pixel optical-input scanner, with the resulting image stored in the computer. Such a digital simulation of a typical halftone image is shown in Figure 10a (with a magnification of three for demonstration purposes). Notice the dot pattern of the background, which is not present in most continuous-tone images. This image was printed by a 400 dots-per-inch printer. Figures 10b and 10c show the result of a 30:1 compression of Figure 10a, using both the signal-dependent QMF filters and the JPEG compression. Notice that the QMF compression attenuates the dot pattern associated with the original. This is because the high detail content of the dot pattern is lost in the QMF compression. In this instance, attenuation has become an asset, actually improving the appearance of the image. The JPEG-compressed image seems to produce a noise pattern in the output. This is indicative of the problems faced when using JPEG compression on halftone images.

By utilizing a wavelet technique, it is possible to quantize images with bit rates as low as 0.4 bits per pixel, while maintaining a sufficiently high quality of reconstruction [9].

5. Relevance of discrete-wavelet techniques in computational electromagnetics

There are essentially two different ways to solve operator equations utilizing wavelet techniques. The first possibility is to use the wavelets as basis functions, in a conventional Method-of-Moments formulation. The second approach is to use traditional sub-sectional basis functions, and obtain a dense complex matrix. The wavelet techniques are then used to compress the elements of the matrix, and either a direct sparse solver or an iterative method is used to obtain the solution of the sparse-matrix system. The

basic philosophy of the two methodologies is the same: namely, to obtain a sparse complex matrix instead of a full one, as results utilizing MoM and sub-sectional basis functions. However, the advantage of forming a sparse matrix is offset by the problem that the condition number of the transformed matrix may be worse. This is particularly significant for the second method, where the transformation utilizing a wavelet-like basis, from a complex-full matrix to a sparse-complex matrix, is orthogonal, from a strictly mathematical point of view. However, from a purely numerical perspective, as will be shown later, the results do not confirm this orthogonal transformation, as the condition number of the system changes and, in some cases, the change is by an order of magnitude.

5. 1 Application of wavelet basis for the solution of operator equations

In [22], a Galerkin method, utilizing a wavelet basis, has been used for the analysis of radiation for TM-scattering problems. There, a method is also proposed to compress the impedance matrix, utilizing wavelet techniques. This is accomplished through a compression process in which only the significant terms in the expansion of the (yet unknown) current are retained and subsequently derived.

Wavelet bases have also been used to solve the Fredholm integral equation of the first kind, which leads to the TM-scattering from conducting cylinders [23]. Here, the compactly supported semi-orthogonal bases have been used. The wavelets have been specially constructed for the bounded interval for solving first-kind integral equations. It has been observed that the use of cubic-spline wavelets almost diagonalizes the matrix. Explicit closed-form polynomial representations for the scaling functions and wavelets are given.

In [24], the wavelet-expansion method, in combination with the boundary-element method (BEM), has been used to solve the integral equation for the surface currents. The unknown current is

Figure 10a. The original, simulated halftone picture printed on a 400 dpi digital printer.

Figure 10b. A compressed version of the simulated halftone picture of Figure 10a, utilizing QMF 30:1 compression.

Figure 10c. A compressed version of the simulated halftone picture of Figure 10a, utilizing JPEG 30:1 compression.

expanded in terms of a basis derived from a periodic, orthogonal wavelet in a finite interval. Because the geometrical representation of the BEM is employed to establish the mapping between the curved computational domain and the interval [0,1], it would be very interesting to find out how this can be extended to three-dimensional problems, where an arbitrary surface needs to be discretized.

An adaptive multi-scale Moment Method is presented in [25], for the solution of the Fredholm integral equation of the first kind. An adaptive procedure is outlined, which refines the unknown solution in regions utilizing multi-scale wavelet-like functions. Even though

the matrix is highly sparse, the deterioration in the condition number of the matrix–as opposed to the condition number of the original matrix utilizing a conventional sub-sectional basis–is clearly visible. One disturbing fact is that the results are not consistent with the increase of the order of the filter, nor with the level of thresholding used. The methodology can also be used for solution of the differential form of Maxwell's equations, utilizing finite elements [26]. Similar wavelet-like functions can also be used to compress the elements of the impedance matrix, utilizing a thresholding operation.

In [27], the problem of electromagnetic scattering from perfectly conducting strips, coated with thin dielectric material, is analyzed, utilizing an adaptive multi-scale Moment Method. The method of a non-uniform grid and the multi-scale technique, which generates a locally finer grid, are usually used when the solutions of the integral equations or the differential equations are known to vary widely in different domains. By non-uniform gridding, one can reduce the size of the problem and improve the accuracy. The multi-level or the multi-grid technique has been widely used in solving differential equations and integral equations [28-32]. Kalbasi and Demarest [33, 36] applied multilevel concepts to solve the integral equation by the Moment Method on different levels, which has been called the Multilevel Moment Method. No matter what the multi-grid technique is, the basis functions for an improved approximation have to be reconstructed again. By using the multi-scale technique in one dimension, the basis functions for the new scale have to be reconstructed. The new approximation grids formed by the multi-scale technique are the same as those for the multilevel technique; however, the constructions for the functions are different.

In addition to these numerical concerns, there are some philosophical concerns that need to be addressed in the selection of an appropriate set of basis functions. Consider the solution of an operator equation

$$\mathrm{AX} = \mathrm{Y}, \tag{75}$$

where, in general, A is a known integro-differential operator, and X is the unknown to be solved for a given excitation, Y. For the solution of boundary-value problems, the most widely used techniques, like MoM, FEM, and BEM, convert the functional equation to a matrix equation. The matrix equation is then solved for some unknown constants, instead of obtaining the solution in terms of unknown functions. The solution procedure starts by expanding the unknown, X, in terms of known basis functions $e_i(t)$, with some unknown constant multipliers a_i in front, i.e.,

$$\mathrm{X}(t) \cong \sum_{i=1}^{N} a_i e_i(t). \tag{76}$$

We then substitute Equation (76) into Equation (75), and form the error or the residual (R), defined by

$$\mathrm{R} = \mathrm{Y} - \mathrm{AX} \cong \mathrm{Y} - \mathrm{A}\left[\sum_{i=1}^{N} a_i e_i(t)\right] = \mathrm{Y} - \sum_{i=1}^{N} a_i \,\mathrm{A}\, e_i. \tag{77}$$

Then, the objective is to make the residuals zero with respect to some weighting functions, W_j. From Equation (77), it is quite clear that $\mathrm{A}\, e_i$ must approximate Y in some sense. Hence, it is required that $\mathrm{A}\, e_i$ must be linearly independent, and must form a complete set. It is immaterial whether the e_i are linearly independent, or even orthogonal! This point was illustrated by [13-17], through the solution of the following differential equation:

$$\frac{d^2 y}{dx^2} = \sin x + 2 \text{ for } 0 \le x \le 2\pi, \tag{78}$$

which has a solution $y = -\sin x + x(x - 2\pi)$ when the boundary conditions are $y(x = 0) = 0$ and $y(x = 2\pi) = 0$.

A particular choice of the basis functions e_i for the unknown y could be the Fourier series, i.e.,

$$y = a_0 + \sum_{n=1}^{\infty} (a_n \cos nx + b_n \sin nx), \tag{79}$$

in which the Fourier bases are linearly independent and orthogonal. This yields a solution $y = -\sin x$. Hence, it does not provide the correction solution. This is because the series for $\frac{d^2 y}{dx^2}$, formed after the double differentiation of Equation (79), is not complete, as the a_0 term is missing. So, $\mathrm{A}\, e_i$ does not form a complete set [13-17]. Hence, Equation (79) does not and cannot provide the correct solution. To rectify the error, one should choose the basis functions as [15,16]

$$y = c_0 + c_1 x + c_2 x^2 + \sum_{n=1}^{\infty} (a_n \cos nx + b_n \sin nx). \tag{80}$$

These basis functions are not even linearly independent in the interval 0 to 2π, as both x and x^2 can be approximated by the remainder of the functions representing the Fourier series. However, if we form $\frac{d^2 y}{dx^2}$, we obtain

$$d_0 + \sum_{n=1}^{\infty} (d_n \cos nx + e_n \sin nx),$$

(with $d_0 = 2c_2$, $d_n = -n^2 a_n$, $e_n = n^2 b_n$), which, indeed, form a complete set. Utilizing Equation (76), it is then possible to get the exact solution. This example clearly illustrates that the choice of the bases is important. Moreover, it is not necessary for the basis functions e_i to be orthogonal or even complete. What is necessary is that $\mathrm{A}\, e_i$ must form an orthogonal set [13-17]. Hence, it is necessary to address the question, how does the set $\mathrm{A}\, e_i$ form a complete set when one chooses a wavelet-like basis?!

For the wavelet methodology to be successful, the wavelet techniques have to ensure that the wavelet decomposition is carried out for $\mathrm{A}\, e_i$, and not for e_i. This is perhaps extremely difficult to do. Also, it needs to be rigorously shown that all the nice properties of perfect reconstruction, using the wavelets described earlier, remains valid after a couple of differentiations of the series, presumably carried out term by term. Another hurdle is how to extend the one-dimensional technique to two-dimensional and three-dimensional problems. These are open problems.

In this first Section 5.1, we described how to use the wavelets as basis functions in the conventional MoM problems leading to sparse matrices. Also, in [26], how to use this approach for implementation of the differential form of Maxwell's equations utilizing

finite elements has been illustrated. Initial results illustrate how to use the wavelet techniques to generate a sparse matrix, utilizing a wavelet-like basis. A similar methodology can also be used in making sparse matrices–arising in the implementation of finite elements in the solution of differential forms of Maxwell's equations–still sparser.

In the next Section 5.2, how to use the discrete wavelet techniques to transform a complex dense matrix, arising in conventional MoM, into a sparse matrix, utilizing a set of orthogonal transformations, is illustrated. Some work [35-38] has already been done to address this topic. This is described next.

5.2 Solution of large matrix equations by the discrete wavelet transform

Consider the solution of a matrix equation $[\mathrm{A}][\mathrm{X}]=[\mathrm{Y}]$, where $[\mathrm{A}]$ is a known $Q\times Q$ matrix, $[\mathrm{Y}]$ is a known $Q\times 1$ vector, and $[\mathrm{X}]$ is the unknown to be solved for. Note that Q has to be an integer power of two for the wavelet techniques to be applicable. If the original matrix $[\mathrm{A}]$ is not of size 2^m, then the matrix $[\mathrm{A}]$ can be augmented by a diagonal identity matrix to make it 2^m. First, we illustrate how to obtain the wavelet transform of a vector $[\mathrm{Y}]$, and then we will illustrate how to take the wavelet transforms of a matrix $[\mathrm{A}]$. We first select $h'(n)$. We then use $h'(n)$ and $g'(n)$ to find the discrete wavelet coefficients, utilizing Equations (70a) and (70b). What is going to be different is that we are going to express Equations (70a) and (70b) as circular correlations with respect to $h'(n)$ and $g'(n)$, or as circular convolutions with respect to $h(n)$ and $g(n)$, respectively. This is a computationally efficient way to carry out convolution by utilizing the FFT. As an example, we first create the following 8×8 orthogonal matrix $[\mathrm{P}]$ as

$$[\mathrm{P}]=\left[\begin{array}{cccccccc} h'_0 & h'_1 & h'_2 & h'_3 & h'_4 & h'_5 & 0 & 0 \\ 0 & 0 & h'_0 & h'_1 & h'_2 & h'_3 & h'_4 & h'_5 \\ h'_4 & h'_5 & 0 & 0 & h'_0 & h'_1 & h'_2 & h'_3 \\ h'_2 & h'_3 & h'_4 & h'_5 & 0 & 0 & h'_0 & h'_1 \\ \hline -h'_5 & +h'_4 & -h'_3 & +h'_2 & -h'_1 & +h'_0 & 0 & 0 \\ 0 & 0 & -h'_5 & +h'_4 & -h'_3 & +h'_2 & -h'_1 & h'_0 \\ -h'_1 & +h'_0 & 0 & 0 & -h'_5 & +h'_4 & -h'_3 & +h'_2 \\ -h'_3 & +h'_2 & -h'_1 & h'_0 & 0 & 0 & -h'_5 & +h'_4 \end{array}\right] \tag{81}$$

$$=\left[\begin{array}{cccccccc} h_5 & h_4 & h_3 & h_2 & h_1 & h_0 & 0 & 0 \\ 0 & 0 & h_5 & h_4 & h_3 & h_2 & h_1 & h_0 \\ h_1 & h_0 & 0 & 0 & h_5 & h_4 & h_3 & h_2 \\ h_3 & h_2 & h_1 & h_0 & 0 & 0 & h_5 & h_4 \\ \hline -h_0 & +h_1 & -h_2 & +h_3 & -h_4 & +h_5 & 0 & 0 \\ 0 & 0 & -h_0 & +h_1 & -h_2 & +h_3 & -h_4 & +h_5 \\ -h_4 & +h_5 & 0 & 0 & -h_0 & +h_1 & -h_2 & +h_3 \\ -h_2 & +h_3 & -h_4 & +h_5 & 0 & 0 & -h_0 & +h_1 \end{array}\right].$$

[In Equation (81), we have used h_k to represent $h(k)$, to conserve space]. This equation is the matrix form of the discrete wavelet transform of Equations (70a) and (70b). Inside $[\mathrm{P}]$ we have the filter coefficients, six in number. Please note that the first four rows are due to the filters $h'(n)$, and the last four rows are due to $g'(n)$ (see Equation (17) for the relationship between $h'(n)$ and $g'(n)$). Therefore, multiplying a vector (say $[\mathrm{Y}]$) by $[\mathrm{P}]$ is equivalent to filtering (in the transmitted portion) in Figure 1, followed by a sub-sampling of two. The matrix-vector product yields $u(n)$ and $v(n)$. The first four elements are equivalent to $u(n)$ and the last four are $v(n)$. The matrix-vector product has already incorporated the sub-sampling by a factor of two. The sub-sampling by a factor of two is accomplished by the shift between the elements of each row of the matrix $[\mathrm{P}]$. Now, for $[\mathrm{P}]$ to be an orthogonal matrix, it is necessary that the following three equations, similar to Equation (29) [the normalization constant is set to unity] and Equation (30) [the filter is orthogonal to its two-shifted version] hold:

$$\sum_i h^2(i)=1, \tag{82}$$

$$h(0)h(2)+h(1)h(3)+h(2)h(4)+h(3)h(5)=0, \tag{83}$$

$$h(0)h(4)+h(1)h(5)=0. \tag{84}$$

Finally, from the boundary conditions for the filter, $H(z=1)=\sqrt{2}$ and $G(z=1)=0$, we have

$$h(0)+h(2)+h(4)=\frac{1}{\sqrt{2}}=h(1)+h(3)+h(5). \tag{85}$$

Equations (82)-(85) provide four independent equations, and one needs two more to uniquely solve for the $h(i)$s. If one follows Daubechies' procedure for making the wavelets smooth, one would need the derivatives of $G'^{p}(z=1)=0$ for $p=1$ and $p=2$, leading to (from Equation (18))

$$-0\cdot h(0)+1h(1)+2h(2)+3h(3)-4h(4)+5h(5)=0, \tag{86}$$

$$-0\cdot h(0)+1h(1)-4h(2)+9h(3)-16h(4)+25h(5)=0. \tag{87}$$

The setting of the higher-order moments of $g'(n)$ to zero guarantees the smoothness of the wavelets. This, in turn, provides a recipe so that the discrete-wavelet coefficients of the transform drop off rapidly, as one goes to the dilated scales from a fine scale. The number of zeros of $G'^{p}(z)$ at $z=1$ tells us how many basis functions are needed in Equation (55) for approximating $x(t)$. The smoother the function and the higher the order of zeros, the faster the expansion coefficients go to zero, and the fewer coefficients we need to keep. For piecewise functions, a wavelet basis is better. These piecewise functions may have jumps. They may be smooth and then suddenly rough. We keep more coefficients in the rough neighborhoods by going to a smaller scale 2^{-j}. The mesh adapts to $x(t)$ in a way that Fourier methodology finds difficult.

If $x(t)$ has p derivatives, its wavelet coefficients decay like 2^{-np} [38]:

$$|d_{k,n}|=\left|\int x(t)\psi_{n,k}(t)dt\right|\le J2^{-np}\left\|x^{(p)}(t)\right\|,$$

where J is a constant, and $x^{(p)}(t)$ represents the pth derivative of $x(t)$.

However, since we are dealing with a finite number of terms, the drop-off rate of the wavelet coefficients is of little significance. The solution of the above equations can be obtained analytically, and has been given by Daubechies [1] as

$$h(5) = h'(0) = \frac{1+\sqrt{10}+\sqrt{5+2\sqrt{10}}}{16\sqrt{2}}, \tag{88a}$$

$$h(4) = h'(1) = \frac{5+\sqrt{10}+3\sqrt{5+2\sqrt{10}}}{16\sqrt{2}}, \tag{88b}$$

$$h(3) = h'(2) = \frac{10-2\sqrt{10}+2\sqrt{5+2\sqrt{10}}}{16\sqrt{2}}, \tag{88c}$$

$$h(2) = h'(3) = \frac{10-2\sqrt{10}-2\sqrt{5+2\sqrt{10}}}{16\sqrt{2}}, \tag{88d}$$

$$h(1) = h'(4) = \frac{5+\sqrt{10}-3\sqrt{5+2\sqrt{10}}}{16\sqrt{2}}, \tag{88e}$$

$$h(0) = h'(5) = \frac{1+\sqrt{10}-\sqrt{5+2\sqrt{10}}}{16\sqrt{2}}. \tag{88f}$$

Once the filters are available, one can form the orthogonal matrix $[\mathrm{P}]$ by substituting in the above values of h. Let us say we have a vector $[\mathrm{Y_1}]$, of length $Q = 2^5 = 32$. We now know how to extend the wavelet transform to $[\mathrm{Y_1}]$. We create a $[\mathrm{P_1}]$ matrix, which is 32×32, and only six elements of any of its rows are populated by the elements of Equation (88); and a matrix of size 32×32, similar to Equation (81), is also formed. 26 elements per row of the matrix are zero. Note that the first 16 rows of $[\mathrm{P_1}]$ are formed by $h'(m)$, and the last sixteen rows, by $g'(m)$. We pre-multiply $[\mathrm{Y_1}]$ by $[\mathrm{P_1}]$, and obtain a vector $[\mathrm{Y_2}]$. The last 16 elements of $[\mathrm{Y_2}]$ are $d_{k,0}$, and they are fixed. This is the result of filtering $[\mathrm{Y_1}]$ by $g(n)$, in Figure 5. We pre-multiply the first 16 elements of $[\mathrm{Y_2}]$, i.e., $[\mathrm{Y_2'}]$ as shown in Figure 11, by an orthogonal matrix $[\mathrm{P_2}]$, which is 16×16. Again, only six of the elements of any row of matrix $[\mathrm{P_2}]$ are nonzero. The result will be a vector $[\mathrm{Y_3}]$ of 16 elements. The last eight elements are fixed, as they are $d_{k,1}$. The first eight elements of $[\mathrm{Y_3}]$, namely $[\mathrm{Y_3'}]$, are again pre-multiplied by the orthogonal matrix $[\mathrm{P}]$ of Equation (81), as shown in Figure 11, producing $c_{k,2}$ and $d_{k,2}$. The final result is then the wavelet decomposition of the vector $\mathrm{Y_1}$. The resultant composite vector of 32 elements includes the wavelet coefficients resulting from the discrete wavelet transform. It is interesting to note that when dealing with a finite-length vector, the widely presented formula of Equation (55) is no longer applicable. Here we use Equation (71). Instead, we have a series containing both the scaling functions and wavelets. Specifically, for the case we have just considered, we obtain a transformed vector of 32 elements, $[\mathrm{T}]$, which is given by

$$[\mathrm{T}] = \begin{bmatrix} [\mathrm{Y_4'}] \\ [\mathrm{Y_4''}] \\ [\mathrm{Y_3''}] \\ [\mathrm{Y_2''}] \end{bmatrix},$$

$$[\mathrm{P_1}]_{32\times32}[\mathrm{Y_1}]_{32\times1} \rightarrow [\mathrm{Y_2}]_{32\times1} \rightarrow \begin{bmatrix} [\mathrm{Y_2'}] \\ [\mathrm{Y_2''}] \end{bmatrix} \rightarrow \text{wavelet coefficients}$$

$$[\mathrm{P_2}]_{16\times16}[\mathrm{Y_2'}]_{16\times1} \rightarrow [\mathrm{Y_3}]_{16\times1} \rightarrow \begin{bmatrix} [\mathrm{Y_3'}] \\ [\mathrm{Y_3''}] \end{bmatrix} \rightarrow \text{wavelet coefficients}$$

$$[\mathrm{P_3}]_{8\times8}[\mathrm{Y_3'}]_{8\times1} \rightarrow [\mathrm{Y_4}]_{8\times1} \rightarrow \begin{bmatrix} [\mathrm{Y_3'}] \\ [\mathrm{Y_3''}] \end{bmatrix} \begin{matrix} \rightarrow \text{scaling function contribution} \\ \rightarrow \text{wavelet coefficients} \end{matrix}$$

Figure 11. The principles of the wavelet transform, applied to a matrix.

where

$$\mathrm{T}(k) = \begin{cases} c_{k,2} & \text{for } k = 1,\ldots,4 \\ d_{k-4,2} & \text{for } k = 5,\ldots,8 \\ d_{k-8,1} & \text{for } k = 9,\ldots,16 \\ d_{k-16,0} & \text{for } k = 17,\ldots,32 \end{cases}. \tag{89}$$

The coefficients $c_{k,2}$ are due to the scaling functions $\phi_{2,k}$, and the remainder of the coefficients, $d_{k,i}$ $(i = 0,1,2)$ are due to wavelets $\psi_{i,k}$. Note that in this case, even though we have carried out a discrete wavelet transform, we do not need to know anything about the scaling and the wavelet functions $\phi_{2,k}$ and $\psi_{i,k}$. The discrete wavelet transform of $[\mathrm{Y_1}]$ is depicted in Figure 5. The choice of the filter $h'(m)$ completely defines the entire procedure. Also, note that for an infinite sum in Equation (55), we never talk about the scaling function in the summation. However, for the finite-sum case, the wavelets by themselves are not complete. One needs the contribution of the scaling functions. Unfortunately, this very important feature is not spelled out explicitly in the literature.

To compute the inverse of the discrete wavelet transform of the resultant vector, one simply reverses the procedure. In this case, we start with the smallest level of the hierarchy, and work our way through. This is expressed by Equation (74). The inverse matrix of all the $[\mathrm{P}]$s in this case is simply their transpose, as $[\mathrm{P}]$s are real orthogonal matrices. To compute the two-dimensional wavelet transform, one follows the rules of the FFT. One deals with all the rows and then all the columns.

Next, we consider the solution of the matrix equation $[\mathrm{A}][\mathrm{X}] = [\mathrm{Y}]$, utilizing the discrete wavelet transform. The discrete wavelet transform actually does not solve any matrix equations. What the wavelet transform does is to preprocess the matrix $[\mathrm{A}]$ and make it sparse, if some thresholding is applied [31].

The basic principle, as outlined by Beylkin, Rokhlin, and Coifman [18], based on [19], is as follows. Let the matrix elements be generated from a kernel, such that the magnitude of the elements of the matrix $[\mathrm{A}]$ decay from the diagonal as $\frac{1}{|i-j|^{\alpha}}$, where i and j may be the row or the column number. Then, if the two-

dimensional discrete wavelet transform is applied to the system matrix $[A]$, the resulting system matrix will be sparse if all the elements below a threshold are set to zero. Typically, one would have only $10Q\log_{10}\left(\frac{1}{\varepsilon}\right)$ elements in the sparse system, where Q is the size of the matrix and ε is the truncation level, i.e. elements of the resultant matrix whose absolute value is less than ε will be discarded. So, for a 2048×2048 matrix, the resultant system matrix would be sparse by a factor of about 30 [20].

Consider a real matrix $[A]$, of dimension $Q\times Q$, where Q is large. Let the elements of $[A]$ be defined by

$$A(i,j)=\begin{cases}1 & \text{if } i=j\\ \dfrac{1}{\sqrt{|i-j|}} & \text{for } i\neq j\end{cases}. \tag{90}$$

We now apply a wavelet transform to the matrix $[A]$. This is equivalent to pre- and post-multiplying $[A]$ by a number of orthogonal matrices. Let $[S]$ be the product of the orthogonal matrices $[P_i]$, as explained earlier for the one-dimensional discrete wavelet transform explained by Figure 11:

$$[S]=[P]\ldots[P_3][P_2][P_1]. \tag{91}$$

Even though the sizes of the various $[P_i]$s are not the same, we make them the same by supplementing, say, $[P_2]$ by a diagonal unity matrix, $[I]$, to make it the same size as $[P_1]$. Thus,

$$[P_1]=\begin{bmatrix}[P_2]_{k\times k} & 0\\ 0 & [1]_{k\times k}\end{bmatrix}_{2k\times 2k}. \tag{92}$$

Since the product of all orthogonal matrices is an orthogonal matrix, $[S]$ is an orthogonal matrix. When the wavelet transform is applied to the system of equations $[A][X]=[Y]$, one obtains

$$[S][A][S]^T[S][X]=[S][Y], \tag{93}$$

where T denotes the transpose of a matrix. Since $[S]$ is an orthogonal matrix, we have

$$[S]^T[S]=[I], \tag{94}$$

where $[I]$ is the identity matrix. So, we take the wavelet transform of $[X]$ and $[Y]$ to form $[X']$ and $[Y']$, and we take the wavelet transform of $[A]$ to form $[B]$. Hence, Equation (93) reduces to

$$[B][X']=[Y'] \text{ with } [B]=[S][A][S]^T. \tag{95}$$

The unknown $[X]$ is solved for from this by

$$[X]=[S]^T[X']. \tag{96}$$

$[B]$ is the two-dimensional wavelet transform of $[A]$, and has been computed by a series of one-dimensional transforms to its rows and columns, which is similar to carrying out a two-dimensional FFT.

Table 1. The sparseness, error in reconstruction, and condition number of the two-dimensional wavelet transform of a matrix $[A]$ of the form in Equation (90), as a function of the order of the filter, with a threshold of 0.001, $Q=512$, and the condition number of $[A]$ given by $Cond[A]=4.45\times 10^6$.

Order of Filter $N+1$	% of Nonzero Elements	Error in Reconstruction δ	$Cond[B_n]$
4	7.58%	$.58\times 10^{-4}$	4.66×10^6
8	6.28%	$.54\times 10^{-4}$	5.56×10^6
16	6.41%	$.52\times 10^{-4}$	5.74×10^7
32	6.54%	$.51\times 10^{-4}$	1.57×10^7

Table 2. The sparseness, error in reconstruction, and condition number of the two-dimensional wavelet transform of a matrix $[A]$ of the form in Equation (90), as a function of the order of the filter, with a threshold of 0.001, $Q=1024$, and the condition number of $[A]$ given by $Cond[A]=3.02\times 10^7$.

Order of Filter $N+1$	% of Nonzero Elements	Error in Reconstruction δ	$Cond[B_n]$
4	3.88%	$.38\times 10^{-4}$	2.56×10^8
8	3.17%	$.33\times 10^{-4}$	3.69×10^7
16	3.18%	$.33\times 10^{-4}$	8.43×10^7
32	3.10%	$.32\times 10^{-4}$	1.53×10^7

Now, we consider $[A]$ to be of the form in Equation (90), and choose various order filters (i.e., $M=N+1$) for $h(n)$, with 4, 8, 16, or 32 terms. Next, we compute $[B]=[S][A][S]^T$ ($[S]$ being given by Equation (91)), and then apply a threshold to the elements of $[B]$ to obtain matrix $[B_a]$. The matrix $[B_a]$ is an extremely sparse matrix. For example, if the threshold is set at 10^{-3} and the size of $[A]$ is $Q=512$, and if we then apply a fourth-order filter (i.e., $M=N+1=4$) $h(n)$, we find that only 7.58% of the elements of $[B_a]$ are nonzero (see Table 1).

Next, take that sparse matrix $[B_a]$, and try to reconstruct $[A]$ by computing

$$[A_a]=[S]^T[B_a][S]. \tag{97}$$

Define an average value, δ, of the error between the elements of $[A_a]$ and $[A]$ by

$$\delta=\frac{1}{Q^2}\sum_i\sum_j|A_a(i,j)-A(i,j)|. \tag{98}$$

From Tables 1-6, it is seen that the matrix $[A]$ can be recovered from $[B_a]$ to provide $[A_a]$ with an average error that is lower than

Table 3. The sparseness, error in reconstruction, and condition number of the two-dimensional wavelet transform of a matrix $[A]$ of the form in Equation (90), as a function of the order of the filter, with a threshold of 0.001, $Q = 2048$, and the condition number of $[A]$ given by $Cond[A] = 6.80 \times 10^7$.

Order of Filter $N+1$	% of Nonzero Elements	Error in Reconstruction δ	$Cond[B_n]$
4	1.97%	$.24 \times 10^{-4}$	5.01×10^7
8	1.60%	$.20 \times 10^{-4}$	5.48×10^7
16	1.58%	$.19 \times 10^{-4}$	3.29×10^7
32	1.51%	$.19 \times 10^{-4}$	6.61×10^7

Table 4. The sparseness, error in reconstruction, and condition number of the two-dimensional wavelet transform of a matrix $[A]$ of the form in Equation (90), as a function of the order of the filter, with a threshold of 0.0001, $Q = 512$, and the condition number of $[A]$ given by $Cond[A] = 4.45 \times 10^6$.

Order of Filter $N+1$	% of Nonzero Elements	Error in Reconstruction δ	$Cond[B_n]$
4	11.9%	$.78 \times 10^{-5}$	5.03×10^6
8	9.9%	$.63 \times 10^{-5}$	5.84×10^6
16	10.1%	$.61 \times 10^{-5}$	4.59×10^6
32	9.9%	$.53 \times 10^{-5}$	1.12×10^7

Table 5. The sparseness, error in reconstruction, and condition number of the two-dimensional wavelet transform of a matrix $[A]$ of the form in Equation (90), as a function of the order of the filter, with a threshold of 0.0001, $Q = 1024$, and the condition number of $[A]$ given by $Cond[A] = 3.02 \times 10^7$.

Order of Filter $N+1$	% of Nonzero Elements	Error in Reconstruction δ	$Cond[B_n]$
4	6.25%	$.54 \times 10^{-5}$	2.77×10^7
8	5.06%	$.41 \times 10^{-5}$	2.55×10^7
16	5.09%	$.38 \times 10^{-5}$	2.98×10^7
32	4.84%	$.33 \times 10^{-5}$	2.27×10^7

Table 6. The sparseness, error in reconstruction, and condition number of the two-dimensional wavelet transform of a matrix $[A]$ of the form in Equation (90), as a function of the order of the filter, with a threshold of 0.0001, $Q = 2048$, and the condition number of $[A]$ given by $Cond[A] = 6.80 \times 10^7$.

Order of Filter $N+1$	% of Nonzero Elements	Error in Reconstruction δ	$Cond[B_n]$
4	3.20%	$.35 \times 10^{-5}$	5.98×10^7
8	2.56%	$.25 \times 10^{-5}$	5.27×10^7
16	2.55%	$.23 \times 10^{-5}$	6.64×10^7
32	2.36%	$.21 \times 10^{-5}$	4.42×10^7

the value of the threshold used to eliminate the wavelet coefficients of $[A]$, (or, equivalently, the elements of matrix $[B]$). The number of $[P_i]$ matrices (see Equation (92)) used for obtaining the results appearing in Tables 1-6 is $\mathrm{INT}\left[\log_2\left(\frac{Q}{N+1}\right)\right]$ (INT stands for "the integer part of"). Please note that the wavelet transform of a real function is always real.

The other interesting property to note is that utilizing a higher-order filter does not necessarily produce larger sparsity, as shown in Tables 2, 4, and 5.

The computational time in the computation of the wavelet transforms in the compression of a matrix is now investigated. We consider a filter of length $L = N+1$, and the data matrix is of length Q. Then the one-dimensional wavelet transform of $[Y]$ may be done (we carry out the initial product at the highest stage of resolution and then down-sample) by the following number of mathematical operations:

$$QL\left(1+\frac{1}{2}+\frac{1}{4}+\ldots\right) = 2QL. \tag{99}$$

To carry out the two-dimensional wavelet transform of $[A]$, we require $(2QL)^2$ operations. Therefore, to produce the sparse system of Equation (95), we require $4Q^2L^2 + 2QL$ operations, resulting in a matrix $[B]$ that contains, at most, of the order of $O(Q)$ elements. If we now apply the conjugate-gradient method to solve the sparse system, per iteration we will require $O(2Q)$ multiplications to carry out two matrix-vector products. Even if the conjugate-gradient method converges in at most Q steps (where Q is the number of unknowns), then we have solved Equation (95) in an operation count of $QO(2Q)$, in addition to $4Q^2L^2 + 2QL$ operations. Observe that this $O(Q^2)$ is significantly lower than the conventional $Q^3/3$ operations typically required in a solution of a matrix equation of size Q. This is essentially the contribution of Beylkin, Coifman, and Rokhlin [18].

However, it is interesting to note that the nature of the variation $\frac{1}{|i-j|^\alpha}$ may also be the result from a convolution. In that case, the FFT would be much faster than the discrete wavelet transform, as the FFT essentially diagonalizes the operator/matrix. However, for other cases, even when the variation is not due to a convolution, the wavelet result still holds.

The most disturbing fact about the discrete wavelet transform is that the condition number of the matrix changes after the transform. It has been shown earlier that the wavelet transform of the matrix $[A]$, which is $[B]$, has been formed through a series of orthogonal transformations. Therefore, by definition, the condition number of the matrix should not change as one goes from $[A]$ to $[B]$. However, as is clear from the six tables, there is a change in the condition number of the transformed matrix when one uses a different-order filter. Also, the condition number is dependent on the threshold used to truncate the elements. There appears to be a lack of systematic change in the results. In this case, the matrix $[A]$ is real.

As a final example, consider the electromagnetic scattering from an array of wires, randomly spaced. We considered 56 thin-wire antennas. Six were of length 2.7λ and radius 0.005λ. The remaining 50 were 3λ long and of the same radius. The 56 wires were located inside a parallelepiped of dimensions $27\lambda \times 25\lambda \times 21\lambda$. The usual MoM application led to a 2096×2096 matrix. The matrix was compressed, utilizing a filter $h(n)$ of length 16. The compression for the real part of the impedance matrix was 17.8%, i.e. 749289 of the elements of the matrix were above a threshold of 10^{-3}. For the imaginary part of the impedance matrix, only 3.28% of the elements were nonzero. This sparse impedance matrix was then used in a conjugate-gradient routine, to solve the transformed Equation (93). Convergence in the residuals of 10^{-2} was obtained in 95 iterations. This simple example demonstrates the potential for the solution of large matrix equations.

There are a few points that are worth mentioning. First of all, if the compression was not done on the real and the imaginary parts of the matrix separately, then the degree of compression was merely 35%, as opposed to 17.8%. This is significant. Secondly, the size of the impedance matrix has to be a power of two. Thirdly, the conjugate-gradient method takes the same number of iterations (95) to converge to the solution when applied to the original dense matrix, or to the sparse matrix, as the transformation is presumably orthogonal, from a strictly theoretical point of view. However, now as the entire compressed matrix is in memory, the number of page faults is small, and so the result can be obtained quite efficiently.

Note that one of the disadvantages with this procedure is that the size of the matrix Q has to be a power of two for efficient implementation of the wavelet transform.

6. Conclusion

The discrete wavelet transform has been presented from first principles, utilizing the basic concepts of filter theory. It has been shown how to construct the filters $h(m)$ that produce the wavelets and the scaling functions. However, for the discrete case, the introduction of wavelets and scaling functions are not at all necessary. Finally, it has been shown how to apply this technique to the solution of large matrix equations. This was accomplished by compressing a large matrix by means of the discrete wavelet transform. The disturbing point is that the condition number before and after the transform and thresholding is quite different as a function of the order of the filter.

8. Acknowledgment

The contributions of the Editor-in-Chief in helping to prepare this paper for publication are gratefully acknowledged.

9. Appendix 1. The principle of decimation by a factor of two

Pictorially, decimation by a factor of two is represented by the symbol shown in Figure 12, where the decimated signal, $y_D(n)$, has been generated from the original signal, $x(n)$. In the sampled domain, this is equivalent to obtaining the waveform shown in Figure 13. Note that alternate sample values have been dropped. Therefore, from Figure 13, in the sampled domain

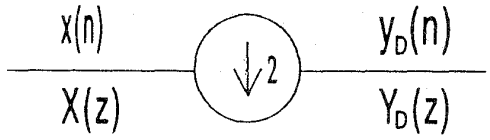

Figure 12. The symbol used to represent decimation by a factor of two.

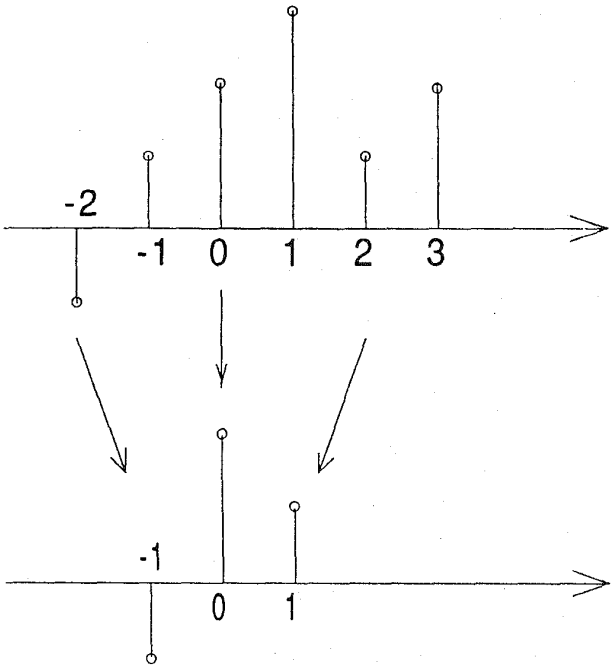

Figure 13. The waveform obtained in the sampled domain from decimation by a factor of two.

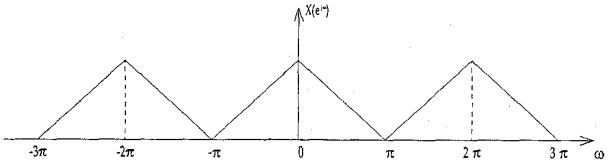

Figure 14. The spectrum of the original signal.

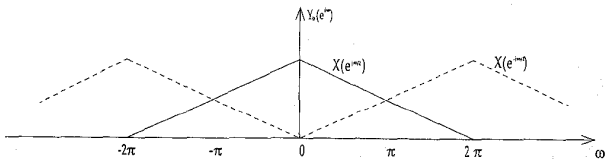

Figure 15. The spectrum of the down-sampled signal.

$$y_D(n) = x(2n),$$

or in the z transform domain,

$$Y_D(z) = \sum_n y_D(n) z^{-n} = \sum_{\text{for } m \text{ even}} x(m) z^{-m/2}$$

$$= \sum_m \frac{x(m)}{2}\left[1+(-1)^m\right]z^{-m/2}$$

$$= \frac{1}{2}\left[X\left(\sqrt{z}\right)+X\left(-\sqrt{z}\right)\right].$$

If we observe the spectrum, then one observes that the original signal has the spectrum given in Figure 14. Once the signal is down-sampled, the spectrum is as given in Figure 15. Hence, the spectrum of $Y_D\left(e^{j\omega}\right)$ is aliased, and it is the sum of

$$Y_D(z) = \frac{X\left(\sqrt{z}\right)+X\left(-\sqrt{z}\right)}{2}.$$

10. Appendix 2. The principle of expansion by a factor of two

Pictorially, up-sampling can be represented by the symbol shown in Figure 16. In the sampled domain, this is equivalent to inserting a zero between the sampled signals, as shown in Figure 17. Mathematically, this is equivalent to

$$y_L(n) = x\left(\frac{n}{2}\right),$$

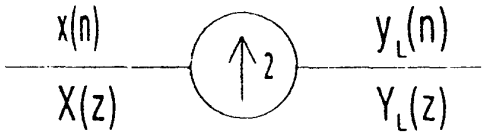

Figure 16. The symbol used to represent up-sampling by a factor of two.

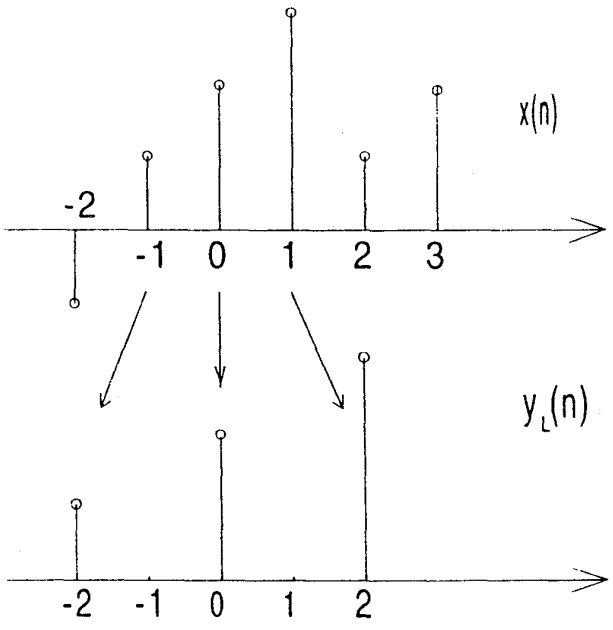

Figure 17. Up-sampling by a factor of two is equivalent to inserting a zero between the sampled signals in the sampled domain.

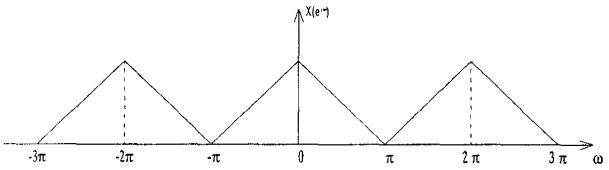

Figure 18. The spectrum of the original signal.

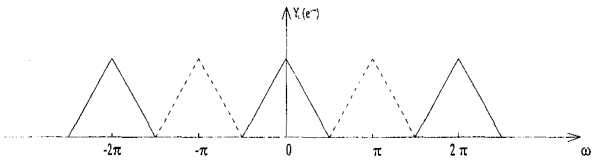

Figure 19. The spectrum of the up-sampled signal.

or, in the transform domain

$$Y_L(z) = \sum_n y_L(n)z^{-n} = \sum_n x\left(\frac{n}{2}\right)z^{-n} = \sum_m x(m)z^{-2m} = X\left(z^2\right).$$

If we observe the spectrum of $Y_L(z)$, then we observe that the original signal in Figure 18 is transformed into the spectrum of Y_2, as shown in Figure 19.

11. References

1. Ingrid Daubechies, *Ten Lectures on Wavelets*, CBMS-NSF Regional Conference Series in Applied Mathematics, Philadelphia, SIAM, 1992.

2. C. K. Chui, *An Introduction to Wavelets*, New York, Academic Press, 1992.

3. P. P. Vaidyanathan, *Multirate Systems and Filter Banks*, Englewood Cliffs, NJ, Prentice-Hall, 1993.

4. J. Morlet, G. Arens, I. Fourgeau and D. Giard, "Wave Propagation and Sampling Theory," *Geophysics*, **47**, 1982, pp. 203-236.

5. Special issue of *IEEE Proceedings*, **84**, 4, April 1996.

6. D. Esteban and C. Galland, "Application of Quadrature Mirror Filters to Split-Band Voice Coding Schemes," Proceedings of the IEEE International Conference on Acoustics, Speech, and Signal Processing, Hartford, Connecticut, 1977, pp. 191-195.

7. M. J. T. Smith and T. P. Barnwell, III, "Exact Reconstruction Techniques for True Structured Subband Coders," *IEEE Transactions on Acoustics, Speech, and Signal Processing*, **ASSP-39**, 1986, pp. 434-441.

8. M. Vettereli, "Multidimensional Subband Coding: Some Theory and Algorithms," *Signal Processing*, **6**, 1984, pp. 97-112.

9. T. H. Koornwinder (ed.), *Wavelets: An Elementary Treatment of Theory and Applications*, New Jersey, World Scientific, 1993.

10. S. Schweid and T. K. Sarkar, "A Sufficiency Criteria for Orthogonal QMF Filters to Ensure Smooth Wavelet Decomposi-

tion," *Applied and Computational Harmonic Analysis*, **2**, 1995, pp. 61-67.

11. S. Schweid and T. K. Sarkar, "Iterative Calculating and Factorization of the Autocorrelation Function of Orthogonal Wavelets with Maximal Vanishing Moments," *IEEE Transactions on Circuits and Systems*, **CAS-42**, 11, November 1995, pp. 694-701.

12. R. Ansari, C. Guillemot and J. F. Kaiser, "Wavelet Construction Using Lagrange Half-Band Filter," *IEEE Transactions on Circuits and Systems*, **CAS-38**, 1991, pp. 1116-1118.

13. M. A. Krasnoselskii, G. N. Vainikko, P. P. Zabreiko, Ya B. Rutitskii and V. Ya Stetsenko, *Approximate Solution of Operator Equations*, Groningen, The Netherlands, Walters-Noordhoff, 1972.

14. S. G. Mikhlin, *The Numerical Performance of Variational Methods*, Groningen, The Netherlands; Walters Noordhoff, 1971.

15. K. Rektorys, *Variational Methods in Mathematics, Science and Engineering*, Dordrecht, Holland, D. Reidel Publishing Company, 1975.

16. T. K. Sarkar, "A Note on the Choice of Weighting Functional in the Method of Moments," *IEEE Transactions on Antennas and Propagation*, **AP-33**, 4, April 1985, pp. 436-441.

17. T. K. Sarkar, A. R. Djordjevic and E. Arvas, "On the Choice of Expansion and Weighting Functions in the Numerical Solution of Operator Equation," *IEEE Transactions on Antennas and Propagation*, **AP-33**, 9, September 1985, pp. 988-996.

18. G. Beylkin, R. Coifman and V. Rokhlin, "Fast Wave Transforms and Numerical Algorithms," *Communications on Pure and Applied Mathematics*, **44**, pp. 141-183.

19. A. P. Calderon, "Intermediate Spaces and Interpolation, the Complex Method," *Stud. Math.*, **24**, 1964, pp. 113-190.

20. W. H. Press, S, Teukolsky, W. T. Vetterling and B. P. Flemery, *Numerical Recipes–The Art of Scientific Computing*, Cambridge, Cambridge University Press, 1992.

21. S. C. Schweid, "Projection Method Minimization Techniques for Smooth Multistage QMF Filter Decompositions," PhD thesis, Syracuse University, May 1994.

22. B. Z. Steinberg and Y. Leviatan, "On the Use of Wavelet Expansions in the Method of Moments," *IEEE Transactions on Antennas and Propagation*, **AP-41**, 5, 1993, pp. 610-619.

23. J. C. Goswami, A. K. Chan and C. K. Chui, "On Solving First-Kind Integral Equations Using Wavelets on a Bounded Interval," *IEEE Transactions on Antennas and Propagation*, **AP-43**, 6, June 1995, pp. 614-622.

24. G. Wang, "A Hybrid Wavelet Expansion and Boundary Element Analysis of Electromagnetic Scattering from Conducting Object," *IEEE Transactions on Antennas and Propagation*, **AP-43**, 2, February 1995, pp. 170-178.

25. C. Su and T. K. Sarkar, "A Multiscale Moment Method for Solving Fredholm Integral Equation of the First Kind," in J. A. King (ed.), *Reports on Progress in Electromagnetic Research, Volume 17*, Cambridge, Massachusetts, EMW Publishing, 1997, pp. 237-264.

26. T. K. Sarkar, R. S. Adve, L. Castillo and M. Salazar, "Utilization of Wavelet Concepts in Finite Elements for an Efficient Solution of Maxwell's Equations," *Radio Science*, **29**, July 1994, pp. 965-977.

27. C. Su and T. K. Sarkar, "Electromagnetic Scattering from Coated Strips Utilizing the Adaptive Multiscale Moment Method," in J. A. King (ed.), *Reports on Progress in Electromagnetic Research, Volume 18*, Cambridge, Massachusetts, EMW Publishing, 1998, pp. 173-208.

28. A. Brandt, "Multi-level Adaptive Solutions to Boundary Value Problems," *Mathematics of Computation*, **31**, 1997, pp. 330-390.

29. W. Hackbusch, *Multigrid Methods and Applications*, New York, Springer-Verlag, 1985.

30. S. F. McCormick, *Multigrid Methods: Theory, Applications and Supercomputing*, New York, Marcel Dekker, 1988.

31. J. Mandel, "On Multilevel Iterative Methods for Integral Equations of the Second Kind and Related Problems," *Numer. Math.*, **46**, 1985, pp. 147-157.

32. P.W. Hemker and H. Schippers, "Multiple Grid Methods for the Solution of Fredholm Integral Equations of the Second Kind," *Mathematics of Computation*, **36**, 153, 1981.

33. K. Kalbasi and K. R. Demarest, "A Multilevel Enhancement of the Method of Moments," in *Seventh Annual Review of Progress in Applied Computational Electromagnetics*, March 1991, Monterey, California, Naval Postgraduate School, pp. 254-263.

34. K. Kalbasi and K. R. Demarest, "A Multilevel Formulation of the Method of Moments," *IEEE Transactions on Antennas Propagation*, **AP-41**, 5, May 1993, pp. 589-599.

35. Z. Baharav, Y. Leviatan, "Impedance Matrix Compressing Using Adaptively Constructed Basis Functions," *IEEE Transactions on Antennas and Propagation*, **AP-44**, 9, 1996, pp. 1231-1238.

36. R. L. Wagner and W. C. Chew, "A Study of Wavelets for the Solution of Electromagnetic Integral Equations," *IEEE Transactions on Antennas and Propagation*, **AP-43**, 8, 1995, pp. 802-810.

37. F. X. Canning, J. F. School, "Diagonal Preconditioners for the EFIE Using a Wavelet Basis," *IEEE Transactions on Antennas and Propagation*, **AP-44**, 9, 1996, pp. 1239-1246.

38. G. Strang and T. Nguyen, *Wavelet and Filter Banks*, Cambridge, Wellesley-Cambridge Press, 1996.

Introducing Feature Article Authors

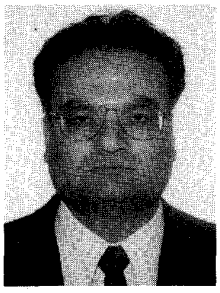

Tapan Kumar Sarkar received the B. Tech. degree from the Indian Institute of Technology, Kharagpur, India, the MScE degree from the University of New Brunswick, Fredericton, Canada, and the MS and PhD degrees from Syracuse University, Syracuse, New York in 1969, 1971, and 1975, respectively.

From 1975 to 1976, he was with the TACO Division of the General Instruments Corporation. From 1976 to 1985, he was with the Rochester Institute of Technology, Rochester, NY. From 1977 to 1978, he was a Research Fellow at the Gordon McKay Laboratory, Harvard University, Cambridge, MA. He is now a Professor in the Department of Electrical and Computer Engineering, Syracuse University; Syracuse, NY. He has authored or co-authored more than 170 journal articles, and has written chapters in ten books. His current research interests deal with numerical solutions of operator equations arising in electromagnetics and signal processing, with application to system design.

Dr. Sarkar is a registered Professional Engineer in the State of New York. He was an Associate Editor for Feature Articles of the *IEEE Antennas and Propagation Society Newsletter*, and he was the Technical Program Chairman for the 1988 IEEE Antennas and Propagation Society International Symposium and URSI Radio Science Meeting. He was the Chairman of the Intercommission Working Group of URSI on Time-Domain Metrology. He is a member of Sigma Xi and USNC/URSI Commissions A and B. He received one of the "best solution" awards in May, 1977, at the Rome Air Development Center (RADC) Spectral Estimation Workshop. He received the Best Paper Award of the *IEEE Transactions on Electromagnetic Compatibility* in 1979, and at the 1997 National Radar Conference. He is a Fellow of the IEEE. He received the degree of Docteur Honoris Causa from the Université Blaise Pascal, Clermont-Ferrand, France, in 1998.

Chaowei Su was born in Jiangsu, People's Republic of China, on April 23, 1961. He received the BS and MSc degrees from Northwestern Polytechnical University (NPU), both in the Department of Applied Mathematics, in 1981 and 1986, respectively. He joined the Department of Applied Mathematics at NPU in 1982. Mr. Su was appointed as an Associate Professor and a full Professor at NPU in 1993 and 1996, respectively. He was a Visiting Scholar at SUNY, Stony Brook, New York, USA, between December, 1990, and June, 1992, supported by a Grumman Fellowship. Since August, 1996, he has been a Visiting Professor at Syracuse University, USA. He is an author of *Numerical Methods in Inverse Problems of Partial Differential Equations and Their Applications* (published by NPU Press). His main research interests are in the area of numerical methods of electromagnetic scattering and inverse scattering, and inverse problems of partial differential equations.

Raviraj S. Adve was born in Bombay, India. He received the BTech degree in electrical engineering from the Indian Institute of Technology, Bombay, in 1990. He is currently working toward the PhD degree at Syracuse University. His research interests include numerical electromagnetics and the use of signal-processing techniques in numerical electromagnetics.

Magdalena Salazar-Palma was born in Granada, Spain. She received the PhD degree in Ingeniero de Telecomunicación from the Universidad Politécnica de Madrid (Spain), where she is a Profesor Titular of the Departamento de Señales, Sistemas y Radiocomunicaciones (Signals, Systems and Radiocommunications Department) at the Escuela Técnica Superior de Ingenieros de Telecomunicación of the same university. She has taught courses on electromagnetic field theory, microwave and antenna theory, circuit networks and filter theory, analog and digital communication systems theory, and numerical methods for electromagnetic field problems, as well as related laboratories. Her research within the Grupo de Microondas y Radar (Microwave and Radar Group) is in the areas of electromagnetic field theory, and computational and numerical methods for microwave structures, passive components, and antenna analysis; design, simulation, optimization, implementation, and measurements of hybrid and monolithic microwave integrated circuits; and network and filter theory and design.

She has authored a total of 10 contributions for chapters and articles in books, 15 papers in international journals, and 75 papers in international symposiums and workshops, plus a number of national publications and reports. She has lectured in several short courses, some of them in the framework of European Community Programs. She has participated in 19 projects and contracts, financed by international, European, and national institutions and companies. She has been a member of the Technical Program Committee of several international symposiums, and has acted as reviewer for international scientific journals. She has assisted the Comisión Interministerial de Ciencia y Tecnología (National Board of Research) in the evaluation of projects. She has also served in several evaluation panels of the Commission of the European Communities. She has acted in the past and is currently acting as topical Editor for the disk of references of the *Review of Radio Science*. She is a member of the editorial board of two scientific journals. She has served as Vice Chair and Chair of the IEEE MTT/AP-S Spanish joint Chapter, and is currently serving as Chair of the Spain Section of the IEEE. She has received two individual research awards from national institutions.

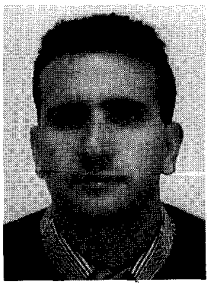

Luis-Emilio García-Castillo was born in 1967 in Madrid, Spain. In 1992. he received the degree of Ingeniero de Telecomu-

nicación from the Universidad Politécnica de Madrid (Spain). In 1993, he became a Research Assistant in the Departamento de Señales, Sistemas y Radiocomunicaciones (Signals, Systems and Radiocommunications Department) in the Escuela Técnica Superior de Ingenieros de Telecomunicación of the same university. Since 1997, he has been an Associate Professor of the Departamento de Ingeniería Audiovisual y de Comunicaciones (Audiovisual and Communications Engineering Department) in the Escuela Univesitaria de Ingeniería Técnica de Telecomunicación of the same university, where he teaches microwave theory and the related laboratory. His research activities and interests are focused on the application of numerical methods, mainly finite elements, to electromagnetic problems, including research on curl-conforming finite elements, the characterization of multiconductor and waveguide structures, analysis of scattering and radiation problems, and the use of wavelet theory in computational electromagnetics. Other research areas of his interest are network theory and filter design.

He has authored four contributions for chapters and articles in books, six papers in international journals, and 29 papers in international symposiums, plus a number of national publications and reports. He has participated in seven projects and contracts financed by international, European, and national institutions and companies.

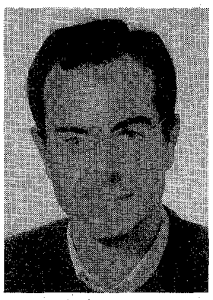

Rafael Rodriguez Boix received the BSc, MSc, and PhD degrees in physics from the University of Seville, Spain, in 1985, 1986, and 1990, respectively. Since 1985, he has been with the Electronics and Electromagnetics Department at the University of Seville, where he became an Associate Professor in 1994. During the summers of 1991 and 1992, he was at the Electrical Engineering Department of UCLA as a Visiting Researcher. Also, during the summer of 1996, he was at the Computer and Electrical Engineering Department of Syracuse University as a Visiting Researcher. His current research activities are focused on the numerical electromagnetic analysis of planar microwave circuits and printed circuit antennas.